REPORT DOCUMENTATION PAGE

Form Approved OMB NO. 0704-0188

1. REPORT DATE (DD-MM-YYYY)	2. REPORT TYPE	3. DATES COVERED (From - To)
29-04-2015	Ph.D. Dissertation	-

4. TITLE AND SUBTITLE
Theory of Multipartite Entanglement for X-Matrices

5a. CONTRACT NUMBER
W911NF-09-1-0385

5b. GRANT NUMBER

5c. PROGRAM ELEMENT NUMBER
611102

6. AUTHORS
S.M. Hashemi Rafsanjani

5d. PROJECT NUMBER

5e. TASK NUMBER

5f. WORK UNIT NUMBER

7. PERFORMING ORGANIZATION NAMES AND ADDRESSES
University of Rochester
518 Hylan Building, RC Box 270140

Rochester, NY 14627 -0140

8. PERFORMING ORGANIZATION REPORT NUMBER

9. SPONSORING/MONITORING AGENCY NAME(S) AND ADDRESS (ES)
U.S. Army Research Office
P.O. Box 12211
Research Triangle Park, NC 27709-2211

10. SPONSOR/MONITOR'S ACRONYM(S)
ARO

11. SPONSOR/MONITOR'S REPORT NUMBER(S)
56228-PH-OC.9

12. DISTRIBUTION AVAILIBILITY STATEMENT
Approved for public release; distribution is unlimited.

13. SUPPLEMENTARY NOTES
The views, opinions and/or findings contained in this report are those of the author(s) and should not contrued as an official Department of the Army position, policy or decision, unless so designated by other documentation.

14. ABSTRACT
In this thesis we focus on the problem of entanglement in an important class of states, called X-states, that we will introduce. Our study led us to an algebraic formula for the value of multipartite entanglement for X-states. We will take advantage of this formula to further explore the connection of entanglement and mixedness in multipartite systems and study the dynamics of entanglement in open systems. We introduce the entanglement, its definition, and the properties of good measures of entanglement in two party and many party systems. This will set the stage for the developments that follow in the thesis.

15. SUBJECT TERMS
X-states, entanglement, open systems, multipartite

16. SECURITY CLASSIFICATION OF:			17. LIMITATION OF ABSTRACT	15. NUMBER OF PAGES	19a. NAME OF RESPONSIBLE PERSON
a. REPORT	b. ABSTRACT	c. THIS PAGE			Joseph Eberly
UU	UU	UU	UU		19b. TELEPHONE NUMBER 585-275-4576

Report Title

Theory of Multipartite Entanglement for X-Matrices

ABSTRACT

In this thesis we focus on the problem of entanglement in an important class of states, called X-states, that we will introduce. Our study led us to an algebraic formula for the value of multipartite entanglement for X-states. We will take advantage of this formula to further explore the connection of entanglement and mixedness in multipartite systems and study the dynamics of entanglement in open systems. We introduce the entanglement, its definition, and the properties of good measures of entanglement in two party and many party systems. This will set the stage for the developments that follow in the thesis.

Theory of Multipartite Entanglement for X-states

by

Seyed Mohammad Hashemi Rafsanjani

Submitted in Partial Fulfillment
of the
Requirements for the Degree
Doctor of Philosophy

Supervised by
Professor Joseph H. Eberly
Department of Physics and Astronomy
The College of
Arts and Sciences

University of Rochester
Rochester, New York

2014

To my parents

Curriculum Vitae

The author was born in Kerman, Iran in 1983. He finished high school and moved to Tehran in 2001 to continue his studies. He finished his undergraduate degree in physics in 2006 and moved to Windsor, Ontario for pursuing his Master's degree. He successfully defended his Master's thesis in 2008 and moved to Rochester, NY, where he has been working ever since pursuing his PhD. The author carried out his doctoral thesis research under the guidance of Professor Joseph Eberly.

Selected Publications

- B.D. Clader and J.H. Eberly, "Modification of short-pulse EIT due to mixed-state medium preparation," in preparation (2008).
- B.D. Clader and J.H. Eberly, "Two-Pulse Propagation in Media with Quantum-Mixed Ground States," Phys. Rev. A 76, 053812 (2007).
- B.D. Clader and J.H. Eberly, "Theoretical study of fast light with short sech pulses in coherent gain media," J. Opt. Soc. Am. B 31, 916 (2007).

- B.D. Clader and J.H. Eberly, "Stimulated Raman Transfer of SIT Solitons," Proc. Int. Symp. on Quant. Opt., Ahmedabad, July 24-27 (2006) (Macmillan of India, 2007).

- B.D. Clader, Q-Han Park, and J.H. Eberly, "Fast light in full coherent gain media," Opt. Lett. 31, 2921 (2006).

- B.D. Clader, Q-Han Park, and J.H. Eberly, "Test of exact solutions for non-EIT fast-light pulses," in Slow and Fast Light 2006 Technical Digest (Optical Society of America, Washington, DC, 2006), TuD5

Acknowledgments

I want to sincerely thank my advisor, Professor Joseph Eberly, for his expert guidance and support for all these years. Your untiring work ethic and strive for perfection is an example that I hope to emulate. I thank Professor Q-Han Park for numerous interesting and stimulating discussions, and for personally teaching me the Park-Shin Bäcklund method, which I use throughout this thesis. I would like to thank the institutions that provided financial support making this work possible. These include the Department of Physics and Astronomy, the Laboratory for Laser Energetics through the Department of Energy funded Frank J. Horton Fellowship, and the National Science Foundation.

I would like to thank my fellow graduate students Ivan Minchev and Jason Nordhaus for their cherished friendship and for providing welcome breaks from studies. I would like to express my wholehearted gratitude to my parents, Timothy and Anna Clader. Finally, I wish to thank my wife Kimberly for her unconditional love and encouragement.

Abstract

We consider the propagation of short, intense laser pulses through media consisting of two-level and three-level atoms. We derive the coupled Maxwell-Bloch (MB) equations, which describe such propagation. Many different physical situations have been studied by analyzing various limiting cases of these equations. Most of the recent work has relied on steady-state or adiabatic assumptions to simplify the analysis of the MB equations. However rapid progress has been made in recent years in developing analytic solution techniques that do not require these simplifications, such as Bäcklund transformations, inverse scattering methods, and Darboux transformations. We use the Bäcklund solution method, to derive soliton solutions to the MB equations for various physical situations of interest in multi-level media. In addition we examine the experimental applicability of the exact solutions by numerically integrating the MB equations for more physically realistic pulse shapes and media preparations that may not permit analytic solutions. In two-level inverted gain media, we derive a pulse solution with group velocity exceeding the speed of light in vacuum (fast light). Numerical results confirm that such a pulse can exhibit fractional peak advances exceeding one pulse width despite spontaneous instabilites such as superfluorescence and stimulated instabilities related to the McCall-Hahn area theorem. In three-level Λ type media we derive soliton solutions for two pulses propagating through a medium prepared in an arbitrary mixed-state of the two ground states. We include a tunable parameter in the solutions that allows one to vary the medium between completely mixed state and completely pure-state superpositions known as "phaseonium". This flexibility allows one to study the interplay between stimulated Raman scattering, electromagnetically induced transparency (EIT), self induced transparency (SIT), and pulse matching. Past results have indicated that asymptotic pulse propagation is always dominated by EIT type propagation when considering two-pulse propagation in phaseonium. Our results indicate that only for pure-state phaseonium does EIT behavior dominate. When one

considers mixed state superpositions of the two ground states, termed "mixonium," asymptotic EIT dominance is replaced with SIT behavior. We show how the area theorem of self-induced transparency appears to govern propagation in both the two and three-level cases.

Contents

List of Figures

Chapter 1

Entanglement and multipartite entanglement

Even though entanglement was already promoted by Schrödinger [1] as a fundamental aspect of quantum theory and in mathematics it predated quantum mechanics by decades [2], only in recent decades it has been recognized that quantum mechanical systems can be used for real world applications of significant importance, including quantum information processing [3, 4], quantum cryptography [5], and quantum metrology [6]. Many of these applications require entanglement between more than two parties; see, e.g., [3, 4]. Such systems also allow us to probe the transition from quantum to classical behaviors in increasingly complex systems [7, 8]. These applications are of sufficient importance to have prompted a number of experimental initiatives for generating entanglement between many parties [9, 10, 11, 12, 13, 14, 8, 15]. Additionally, achieving quantum systems with scalable architectures continues to motivate much research.

In tandem with experimental efforts to create entanglement in many-party systems there has been a theoretical effort aimed at quantifying the entanglement in many party systems. Of particular importance is the entanglement existing collectively between all N parties of an N-party system, which we call all-party entanglement, and which plays an important role in high-precision metrology as well as other applications [6, 16, 17]. Quantifying the entanglement has proved to be a challenging task. only in few-party cases do prescriptions exist for determining the entanglement of a mixed state [18, 19, 20, 21, 22, 23, 24]. In multipartite systems previous

studies have produced witnesses and/or lower bounds of the all-party entanglement [25, 26, 27, 28, 29, 30, 31, 32, 29, 28]. Many of these results are not well suited for use in experimental settings because they apply only for idealized noise-free states [30, 31, 32, 29], require numerical methods only feasible for few-partite systems [28], or require knowledge of the density operator of the state under test [25, 26]. The latter requirement is a problem for multi-party systems because, in general, the number of measurements to determine the density operator scales exponentially with the number of parties [33]. Apart from these methods, the measured value of witness operators can be used to find a lower bound for the entanglement realized in an experiment [34, 35, 36, 37]. Nonetheless, the efficacy of this approach for producing non-trivial lower bounds is not guaranteed, and complementary techniques are desired. In summary, quantifying all-party entanglement remains a challenge.

In this thesis we focus on the problem of entanglement in an important class of states, called X-states, that we will introduce in the following chapter. Our study led us to an algebraic formula for the value of multipartite entanglement for X-states. We will take advantage of this formula to further explore the connection of entanglement and mixedness in multipartite systems and study the dynamics of entanglement in open systems. In the current chapter we introduce the entanglement, its definition, and the properties of good measures of entanglement in two party and many party systems. This will set the stage for the developments that follow in the rest of the thesis.

1.1 Separability and entanglement

Here we start with the definition and examples of two-party entanglement, also known as bipartite entanglement, and in the following section we explain how the definition can be extended to include many-party entanglement. Perhaps the simplest way to define the entanglement is through its opposite: separability. Entanglement implies lack of separability among two or even more parties. To start with the simplest case, think of two parties, A and B, and their joint pure state $|\psi_{AB}\rangle$. Such a state is defined to be a separable state if it can be written as a direct product of two pure states each describing the state of either A or B: $|\psi_{AB}\rangle = |\psi_A\rangle \otimes |\psi_B\rangle$. But if such a decomposition is not possible, then the two parties are entangled. The extension of the idea to include mixed states is quite simple. First think of a convex sum of separable

states. Also assume there is an inequality of the form $F \geq 0$ that cannot be violated for any pure biseparable states and F is a linear function of expectation values of the joint state. Historical examples are the Bell inequalities. Now think of an ensemble of states where each state is a separable pure state with a given probability $\{p_i, |\psi_i\rangle\}$. For each of the pure states from this ensemble $F_i \geq 0$, and thus $\bar{F} = \sum_i p_i F_i \geq 0$. The average, $\bar{F}$, corresponds to the average value of the given ensemble. Note than an such ensemble denotes a mixed state and also each mixed state denotes such an ensemble. Thus if pure separable states cannot violate certain inequalities with the properties given above, their mixtures cannot violate those inequalities either. This is then how we extend the definition of separability to mixed states. A mixed state is separable if and only if it can be written as a convex sum of pure biseparable states. One can readily show that this is equivalent to the way it is presented, that a mixed state ρ is separable iff it can be written as

$$\rho = \sum_i p_i \ \rho_{Ai} \otimes \rho_{Bi} \tag{1.1.1}$$

where ρ_{Ai}'s and ρ_{Bi}'s are density matrices in the Hilbert spaces of A and B respectively. Thus to prove that a given state is entangled one needs to prove that such a decomposition does not exist. Typically that is the difficult part of the problem. Only in special cases are there simple solutions whether such a decomposition exists or not. The problem arises from the fact that for any mixed state there are typically an infinite number of ways to write the density matrix as a convex sum of pure states (pure state decompositions). To determine that none of the pure state decompositions is a sum of pure separable states is typically an open challenge.

For some special cases it is simple to determine whether the state is entangled or separable. One such example is the case of a bipartite pure state. The simplicity is due to the idea of the Schmidt decomposition that was introduced by Schmidt more than a century ago [2]. This was the first treatment of entanglement and in this sense entanglement predates quantum mechanics by three decades. The relevant result is given below.

For any two Hilbert spaces $\mathcal{H}_1$, and $\mathcal{H}_2$, a pure state in the space $\mathcal{H}_1 \otimes \mathcal{H}_2$ can be written as

$$|\psi\rangle = \sum_{i,j} a_{ij} |i\rangle \otimes |j\rangle \tag{1.1.2}$$

where $|i\rangle$, and $|j\rangle$ are orthonormal bases for the two Hilbert spaces. Schmidt showed that such a state can always be written using a sum on a single index

$$|\psi\rangle = \sum_s \sqrt{\lambda_s}|\phi_s\rangle \otimes |\chi_s\rangle \tag{1.1.3}$$

where $\langle\phi_s|\phi_r\rangle = \langle\chi_s|\chi_r\rangle = \delta_{rs}$. This result is equivalent to the singular value decomposition of the matrix a whose elements are a_{ij}. The coefficients λ's are the eigenvalues of each of the reduced density matrices ρ_1, and ρ_2 and their sum is unity. This coefficients are called Schmidt coefficients. Another proof of this result and a brief discussion can be found in [5]. The connection to entanglement becomes readily clear when we notice that for a separable state only a single term contributes to the Schmidt decomposition. Thus any state that has more than one non-zero Schmidt coefficients is entangled. For example a bipartite state such as

$$\frac{1}{\sqrt{2}}|00\rangle + \frac{1}{\sqrt{2}}|11\rangle \tag{1.1.4}$$

is already written in a Schmidt form and its Schmidt coefficients are both $\frac{1}{2}$. Now that for this simple case we learned how to determine whether a state is entangled or separable, another question arise. How to determine how entangled some given state is? For the above case the answer is readily available. One can use the Schmidt weight, K, that is defined below.

$$K = \frac{1}{\sum_i \lambda_i^2} \tag{1.1.5}$$

This value is always larger than one and for example for the above Bell state is 2. It weighs how many modes contribute to the Schmidt sum of the state. But how to find this quantity for a mixed state? or in other words, what is the proper way to extend this definition for mixed states. This leads to a separate question that is what constitutes a good measure of entanglement? In the following section we will discuss this problem and enumerate the properties that a proper measure of entanglement should possess. We then introduce a number of such measures and comment on their connections.

1.2 How to quantify entanglement

Previously we discussed the idea of bipartite entanglement. For the case of pure bipartite states one can use the Schmidt decomposition to determine whether a given state is entangled. The question that arises from the need to quantify the entanglement of a given state. What are the properties that a *good* entanglement measure should possess. Let us name such a measure $E(\rho)$ for the density matrix ρ.

We can readily derive a few immediate properties. The first one is that the measure is positive for all entangled states and zero for all separable states. Now assume that the entangled states is shared by two parties, Alice and Bob. We do not expect that Alice and Bob can create entanglement between them by starting mixing separable states; The mixture of separable states is a separable states. We get a requirement for convexity if we extend the previous assumption to the quantity of entanglement; Mixture of entangled states cannot lead to an entangled state that possesses more entanglement than the average. If $\rho = p\rho_1 + (1-p)\rho_2$

$$E(\rho) \leq p_1 E(\rho_1) + (1-p)E(\rho_2). \tag{1.2.1}$$

The next requirement comes from a similar line of reasoning. Let us first introduce the concept of local operations. These are operators that can be described by operators that belong to the Hilbert space of one of the parties. For example one of the parties may decide to make a measurement in an arbitrary basis of its Hilbert space. The connection to the entanglement comes from the assumption that Local operations cannot increase the entanglement of a state. We do not expect that given a separable state, Alice can perform a local operation on her system that leads to entanglement between her and Bob. Furthermore Alice and Bob cannot use classical communication to coordinate a set of local operations such that on average they end up with higher entanglement than when they started. Thus the measure should be, on average, a non-increasing function under local operations and classical communications (LOCC).

The last requirement deals with a special set of LOCCs, namely local unitary transformations. We expect that entanglement remains invariant under all local unitary transformations. The simplest way to understand this requirement is to note that each local unitary transformation is equivalent to a local change of basis, and the entanglement is the kind of correlation that remains invariant under any choice of basis by Alice (or Bob). A complete discussion on these properties is given [38].

If a function of entanglement satisfies the last three requirements and is zero for all separable states, it is called and entanglement monotone. Note that an entanglement to be a measure of entanglement, however, the measure should also be positive for all entangled states.

We close this section with an important result about making entanglement monotones. Vidal showed in [38] that one can always make entanglement monotones by defining functions that have two properties on the pure states and then extend the definition to mixed states by using a minimization over all pure state decompositions.

Let us assume that the function $f(\sigma)$ is concave over all density matrices, i.e. for $\sigma = p\sigma_1 + (1-p)\sigma_2$ we have $f(\sigma) \geq pf(\sigma_1) + (1-p)f(\sigma_2)$. Furthermore for the function is invariant under all unitary transformations, then the following quantity is invariant under local unitary transformations, an non-increasing under LOCC.

$$F(\rho) = \min \sum_i p_i f(|\psi_i\rangle\langle\psi_i|) \tag{1.2.2}$$

where the minimization is taken over all pure state decompositions of the state. Note that the condition of invariance of $f(\sigma)$ under unitary transformations implies that for pure states the function f depends only on the eigenvalues of any of the reduced density matrices (or Schmidt coefficients).

So far in this section we discussed the properties of a proper measure of entanglement. In the rest of the section we introduce and briefly discuss different examples of the well-known measures of entanglement. Our list is by no means exhaustive but it covers important measures that we will generalize later to the case of multipartite entanglement.

1.2.1 Entanglement of formation

For a bipartite pure state the entanglement of formation is defined by taking the von Neumann entropy of one of the reduced density matrices for each of the parties. This is directly related to the Schmidt coefficients; The entanglement of formation, $E(\Phi)$, is the Shannon entropy of the Schmidt coefficients of the pure state, $|\Phi\rangle$.

$$E(\Phi) = S(\mathrm{Tr}_A|\Phi\rangle\langle\Phi|) = S(\mathrm{Tr}_B|\Phi\rangle\langle\Phi|) \tag{1.2.3}$$

where S denotes the von Neumann entropy. This definition offers an operational interpretation that leads to a natural extension of this definition to the mixed states. It

has been [CITE] shown that in the limit of large n, $nE(\Phi)$ identical copies of a singlet state can be used to produce n copies of the state $|\Phi\rangle$ using only local operations [39, 40]. Thus least number of singlet states required to produce n copies of the state $\rho = \sum_i p_i |\Phi\rangle\langle\Phi|$ is given by $nE(\rho)$ where

$$E(\rho) = \inf \sum_i p_i E(\Phi_i) \tag{1.2.4}$$

where the infimum is taken over all pure state decompositions of ρ. The measure also has all the important properties that are required of a proper measure of entanglement: invariance under local unitary transformation, non-increasing under local operation and classical communication (LOCC), convexity, and strictly positive if and only if for entangled states. The combination of the linear entropy and the optimization over all the pure state decompositions give an operational interpretation to the measure. Yet determining the value of the measure has been elusive. Only when the two parties are two-level systems has the problem been solved analytically. The two-level systems are ubiquitously referred as qubits (short for quantum bits) in quantum information. The solution was proposed in a seminal paper by Wootters [20], in a connection with a new measure of entanglement that we discuss next. It was shown that for any two-qubit state

$$E(\rho) = h(\frac{1 + \sqrt{1 - C(\rho)^2}}{2}) \tag{1.2.5}$$

where $h(x) = -x \log_2 x - (1-x)\log_2(1-x)$, and $C(\rho)$ is the concurrence of the state, that we discuss next.

1.2.2 Concurrence

Here we discuss concurrence and survey some of its properties. We take the historical approach and first discuss the concurrence of two qubits and and then discuss briefly its generalizations to other bipartite states. For a two-qubit pure state the concurrence is defined by

$$C(|\psi\rangle) = |\langle\psi|\sigma_y \otimes \sigma_y|\psi^*\rangle| \tag{1.2.6}$$

where $|\psi^*\rangle$ is the complex conjugate of $|\psi\rangle$ when it is expressed in the basis that diagonalizes σ_z. The extension to mixed states is defined through a minimization over

all pure state decompositions:

$$C(\rho) = \inf \sum_i p_i C(|\psi_i\rangle). \tag{1.2.7}$$

It was shown in [20] that the above quantity can be calculated from

$$C(\rho) = \max\{0, \sqrt{\lambda_1} - \sqrt{\lambda_2} - \sqrt{\lambda_3} - \sqrt{\lambda_4}\} \tag{1.2.8}$$

where the λs are the eigenvalues, in the decreasing order, of the following matrix:

$$\rho(\sigma_y \otimes \sigma_y)\rho^*\sigma_y \otimes \sigma_y \tag{1.2.9}$$

We will sketch the proof below but a complete proof can be found in the original paper [20] and an extended discussion on the proof can be found here [41]. First note that every pure state decomposition of any density matrix $\rho = \sum_i p_i|\psi_i\rangle\langle\psi_i|$ can be found using the following prescription [42]. Let us first subnormalize the states of the ensemble such that $|\Psi_i\rangle = \sqrt{p_i}|\psi_i\rangle$ and we can write the density matrix as $\sum_i |\Psi_i\rangle\langle\Psi_i|$. We define a unitary transformation such that

$$|\Phi_j\rangle = \sum_j V_{ji}|\Psi_i\rangle, \quad \sum_i V_{ki}^\dagger V_{ij} = \delta_{jk}, \tag{1.2.10}$$

One can show that $\rho = \sum_i |\Psi_i\rangle\langle\Psi_i| = \sum_i |\Phi_i\rangle\langle\Phi_i|$. It is shown in [42] that the converse is also true. All pure state decompositions of the density matrix can be related to another using such a unitary transformation. Thus the optimization over all pure state decompositions can be captured by the optimization over all such unitary transformations. The other important part of the proof is the following lemma.

Lemma: If τ is a complex symmetric matrix, $c = \inf_V \sum_i |[V\tau V^T]_{ii}|$ is given by

$$c = \max(0, 2S_1 - \sum_i S_i) \tag{1.2.11}$$

where S_i's are the singular values of the matrix τ, which are equal to eigenvalues of $\tau\tau^\dagger$, in the decreasing order.

Having these two results one can define $\tau_{ij} = \langle\psi_j^*|(\sigma_y \otimes \sigma_y)|\psi_i\rangle$ which is a symmetric

matrix. Then use the following relation

$$C(\rho) = \inf_V \sum_i |\sum_{jk} V_{ij}\tau_{jk}V_{ki}^T| = \inf_V \sum_i |[V\tau V^T]_{ii}| \tag{1.2.12}$$

Finally one uses the lemma we introduced above and prove the formula for the concurrence of a two-qubit matrix.

Concurrence can also be generalized to bipartite systems of higher dimensions. The connection can be established by noting that for a pure state the concurrence can be written as

$$C(|\psi\rangle) = \sqrt{2(1 - \mathrm{Tr}[\rho_A^2])} \tag{1.2.13}$$

where ρ_A is either of the reduced density matrices that one can define for a bipartite pure state. This generalization was first proposed by Rungta *et al.* [43] through the generalization of the spin-flip operator to higher dimensions. One can check that the function satisfies the condition of concavity and invariance under unitary transformations and thus its minimization over all pure state decompositions givens a proper measure of entanglement.

1.2.3 Negativity

Negativity as a measure of entanglement is directly connected with the idea of the positive partial transpose (PPT) criterion that was laid out by Peres [18]. A general bipartite state of the Hilbert space $\mathcal{H}_A \otimes \mathcal{H}_B$ can be always written as

$$\rho = \sum_{ijlk} \rho_{ij,kl}|i\rangle \otimes |j\rangle\langle k| \otimes \langle l| = \sum_{ijlk} \rho_{ij,kl}|i\rangle\langle k| \otimes |j\rangle\langle l| \tag{1.2.14}$$

Now one can define the operation of partial transposition by performing the transposition only on one of the parties, e.g. B:

$$\rho^{T_B} = \sum_{ijlk} \rho_{ij,kl}|i\rangle\langle k| \otimes (|j\rangle\langle l|)^{T_B} = \sum_{ijlk} \rho_{ij,kl}|i\rangle\langle k| \otimes (|l\rangle\langle j|) \tag{1.2.15}$$

Transposition is a positive map but not a completely positive mapping [5]. That means when a positive matrix in a given Hilbert, e.g. $\mathcal{H}_A$ space is transposed, the resulting matrix is always a positive matrix. But if an state is in a product space, $\mathcal{H}_A \otimes \mathcal{H}_B$ and

we apply transposition only to one of the Hilbert spaces, the result is not necessarily a positive matrix. This property has a very important implication when applied to a separable state. A separable state can always be written as

$$\rho_{sep} = \sum_i p_i \rho_{Ai} \otimes \rho_{Bi} \tag{1.2.16}$$

When we apply partial transposition on the state we get

$$\rho_{sep}^{T_B} = \sum_i p_i \rho_{Ai} \otimes \rho_{Bi}^{T_B} \tag{1.2.17}$$

Since ρ_{Bi} is a positive matrix in the Hilbert space $\mathcal{H}_B$ its transpose is a positive matrix too. This implies that $\rho_{sep}^{T_B}$ is also a positive matrix too. Thus if the partial transpose of a state is not a positive matrix, i.e. has at least one negative eigenvalue, the state cannot be a separable state and thus is entangled. Note that the converse is not necessarily true. There exist entangled states whose partial transpose are positive matrices. However, Horodecki [19] showed that for two-qubit and two-qutrit states, the converse is also true and the positivity of the partial transpose is the necessary and sufficient condition for separability.

Negativity also quantifies how far from positivity the partially transposed state becomes. It is defined to be sum of the absolute values of the negative eigenvalues of the partially transposed matrix.

$$\mathcal{N}(\rho) = \frac{||\rho^{T_B}|| - 1}{2} \tag{1.2.18}$$

and as expected vanishes for all separable states. Vidal and Werner showed that negativity is an entanglement monotone [44]. The proof extends beyond the case of two qubits and two qutrits but the positivity of the partial transpose is only a necessary condition for separability. For an extended discussion on negativity one can look in [4].

1.2.4 Distance measures

The last approach to quantify entanglement that we discuss here is the distance approach. It is based on the notion that separable states are convex subspaces, i.e. the convex sum of any two separable state is a separable state. Thus we may quantify the entanglement by the distance of the given state to the set of separable states. The

benefit of this approach is the unifying perspective that it offers. It puts all different quantum correlation such as quantum discord, classicality, entanglement, and etc on the same footing by defining them through the distance of a given state to the corresponding set of states [45].

The immediate draw back is that computing a value for such measures is typically an open issue even for pure states. In the current work we will introduce a distance measure of genuinely multipartite entanglement and will evaluate it for the class of GHZ-diagonal states.

1.3 Multipartite entanglement

Having discussed separability and entanglement between two parties, we next turn to the case of when more than two parties can share entanglement. The first step is to clarify what kind of multipartite entanglement we are going to deal with. Below we present three example states, each can be argued to be entangled.

$$|GHZ_3\rangle = \frac{|000\rangle + |000\rangle}{\sqrt{2}} \tag{1.3.1}$$

$$|W_3\rangle = \frac{|001\rangle + |010\rangle + |100\rangle}{\sqrt{3}} \tag{1.3.2}$$

$$|\chi\rangle = |0\rangle \otimes \frac{|00\rangle + |11\rangle}{\sqrt{2}} \tag{1.3.3}$$

For the first two states it is impossible to separate any part of the system and associate with it a pure state, but for the last example one of the parties is associated with a pure state. Yet even for the last example two of the parties cannot be separated from each other. This brings us to the next definition that allows us to classify different inseparabilities of an N-partite system.

We start with a pure state of N parties. A pure state of N parties is called k-separable if and only if it can be written as a direct product of k separate pure states [46]:

$$|\psi_1\rangle \otimes |\psi_2\rangle \otimes \cdots |\psi_k\rangle \tag{1.3.4}$$

The extension to mixed states follows immediately too. A mixed state of N parties is k-separable if it can be written as a pure state decomposition of k-separable states. Two immediate extremes follow the above definition naturally. First is the case of

N-separability. In that case the state can be written as

$$\sum_i p_i \ \rho_{1i} \otimes \rho_{2i} \otimes \cdots \rho_{Ni} \tag{1.3.5}$$

Such states are more generally referred to as fully separable states. In the current work we refer to the lack of full separability as weak inseparability. The other extreme is when a state is not even 2-separable (biseparabe). This kind of entanglement is referred to as genuinely N-partite entanglement. Sometimes it is also referred to as genuinely multipartite entanglement. Below we discuss this entanglement in more detail.

1.3.1 All-party entanglement

As mentioned entanglement among more than two parties can signal separability among many different partitions of the system. One extreme kind of entanglement is the idea of genuinely multipartite entanglement. Before discussing the concept let us mention that we refer to genuinely multipartite entanglement simply as all-party entanglement. It is because although a term such as genuinely N-partite entanglement is specific enough to refer to the special kind of entanglement that we are concerned with, the term genuinely multipartite entanglement lacks such specificity. Our choice, all-party entanglement, has the advantage that it refers to the specific form of multipartite entanglement we are interested in, as well as the name does not need to be changed for different number of parties. For a three party system, all-party entanglement implies genuinely three-partite entanglement and for a four party system it implies genuinely four-partite entanglement.

All-party entanglement is defined by its opposite, biseparability. A pure N-partite system $|\psi\rangle \in \mathcal{H}_1 \otimes \mathcal{H}_2 \cdots \otimes \mathcal{H}_N$ is biseparable if there is a bipartition of the N parties $\mathcal{H}_1 \otimes \mathcal{H}_2 \cdots \otimes \mathcal{H}_N = \mathcal{H}_A \otimes \mathcal{H}_B$, where $\mathcal{H}_A = \mathcal{H}_{j_1} \otimes \mathcal{H}_{j_2} \otimes \cdots \otimes \mathcal{H}_{j_k}$, $\mathcal{H}_B = \mathcal{H}_{j_{k+1}} \otimes \mathcal{H}_{j_{k+2}} \otimes \cdots \otimes \mathcal{H}_{j_N}$ for which $|\psi\rangle = |\psi_A\rangle \otimes |\psi_B\rangle$, and $|\psi_A\rangle \in \mathcal{H}_A$ and $|\psi_B\rangle \in \mathcal{H}_B$ [47, 4]. In other words, a pure state is biseparable if it has at least one pure marginal (reduced density matrix). An N-partite state that cannot be written as an ensemble of biseparable states is an all-party entangled state.

let us introduce the set of all bipartitions of N parties. Each bipartition is a division of the set $\{1, 2, \ldots, N\}$ into two disjoint and non-empty subsets. The set of all such bipartitions is denoted by $J = \{J_1, J_2, \ldots J_{2^{N-1}-1}\}$. For example for $N = 3$,

there are three bipartitions $J_1 = \{1|2,3\},\ J_2 = \{2|1,3\},$ and $J_3 = \{3|2,1\}$, so that $J = \{J_1, J_2, J_3\}$.

For a pure state $|\psi\rangle$, to each of the elements of J we can associate two reduced density matrices $\hat{A}(|\psi\rangle, J_j)$, and $\hat{B}(|\psi\rangle, J_j)$ by tracing out either of the subsystems associated with that bipartition. The biseparability of a pure state can be determined by whether for any of the elements of J, $\hat{A}(|\psi\rangle, J_j)$ and $\hat{B}(|\psi\rangle, J_j)$ are pure. If so, $|\psi\rangle$ is biseparable. Thus the purity of the jth bipartition, denoted by $\Pi_j(|\psi\rangle)$, is a key parameter.

To determine whether a mixed state $\hat{\rho}$ is biseparable, one has to determine whether $\hat{\rho}$ can be written as a convex sum of pure biseparable states. Thus one has to check all the ways $\hat{\rho}$ can be written as a convex sum of pure states (all pure state decompositions). If it is impossible to write the density matrix of the state as a convex sum of biseparable states then the state is called all-party entangled. Similarly to the case of bipartite case, the mathematical difficulty in ruling out such a biseparable decomposition is the main obstacle in determining whether a state is entangled or biseparable.

1.4 All party concurrence

In this section we discuss the all-party concurrence. We will define it and show that it is a proper measure of all-party entanglement. all-party concurrence is based on previous works by Pope and Milburn [48] and Love, *et al.* [49]. It is formally introduced in the work of Ma *et al.* [26] and it was shown to be a proper measure of entanglement. This measure reduces to the Wootters concurrence [20] for two qubits.

To introduce the measure we use the definition for a pure state. Remember that purity of each partition is a key parameter in determining whether the system is separable along that bipartition. For a pure state GM concurrence is then defined [26] as,

$$C_{GM}(|\psi\rangle) := \min_j \sqrt{2}\sqrt{1 - \Pi_j(|\psi\rangle)}.$$

Clearly, $C_{GM}(|\psi\rangle) \geq 0$ and it is equal to zero if and only if $|\psi\rangle$ is a biseparable state. For a bipartite system this definition reduces to the I-concurrence [43].

To determine whether a mixed state $\hat{\rho}$ is biseparable, one has to determine whether $\hat{\rho}$ can be written as a convex sum of pure biseparable states. Thus one has to check

all the ways $\hat{\rho}$ can be written as a convex sum of pure states (all pure state decompositions). Let us distinguish different pure state decompositions of $\hat{\rho}$ by assigning a continuous superscript, α, to label them:

$$\hat{\rho} = \sum_i p_i^{(\alpha)} |\psi_i^\alpha\rangle\langle\psi_i^\alpha|. \tag{1.4.1}$$

To determine whether a particular pure state decomposition is a sum of biseparable states, we can calculate the average pure state GM concurrence for that particular α

$$\begin{aligned} C_\alpha(\hat{\rho}) &= \sum_i p_i^{(\alpha)} C_{GM}(|\psi_i^\alpha\rangle) \\ &= \sum_i p_i^{(\alpha)} \left\{ \min_j \sqrt{2}\sqrt{1 - \Pi_j(|\psi_i^\alpha\rangle)} \right\}. \end{aligned} \tag{1.4.2}$$

Now we are ready to extend the definition of GM concurrence to all mixed states:

$$C_{GM}(\hat{\rho}) = \min_\alpha \; C_\alpha(\hat{\rho}). \tag{1.4.3}$$

If $C_{GM}(\hat{\rho}) = 0$ this means that there is an α for which $C_\alpha(\hat{\rho}) = 0$. Then $\hat{\rho}$ can be written as a sum of pure biseparable states, so $\hat{\rho}$ is biseparable. If $C_{GM}(\hat{\rho}) > 0$, there is no α for which the $|\psi_i^\alpha\rangle$'s are all biseparable and thus $\hat{\rho}$ is an N-partite entangled state. The all-party concurrence of N parties, as defined in Ref. [26], is a monotone of all-party entanglement. To show that our all-party concurrence is a proper measure of entanglement we need to prove that it satisfies the following properties.

1. It is non-negative and, it is positive *iff* the state is all-party entangled.
2. It is invariant under local unitary transformations.
3. It is convex, i.e. $C_{GM}(\sum_i p_i \hat{\rho}_i) \leq \sum_i p_i C_{GM}(\hat{\rho}_i)$.
4. It is non-increasing under local operations and classical communications.

We have already shown that the first property is satisfied for our measure. The second property follows immediately since purity remains invariant under unitary transformations. Convexity of the measure can be inferred from the fact that the concurrence is the minimum over all pure state decompositions and if $\hat{\rho}$ can be written as a convex sum of some other density matrices, then the convex sum of the optimal pure state decompositions of matrices in the sum is itself a pure state decomposition of $\hat{\rho}$. Hence

the convexity follows. Thus remain the last property. Note that for each bipartition the I concurrence is non-increasing under LOCC and since all-party concurrence is the minimum over all these bipartitions then it should be non-increasing too. Finally we note that, the operational meaning of GM concurrence in terms of mutual information is explicitly discussed in Ref. [50].

1.5 Chapter summary and what is to follow

In this chapter we examined entanglement and its different properties in two different context. First we surveyed entanglement between two parties. We started with the Schmidt decomposition to clarify the mathematical definition of entanglement between two parties that are sharing a pure state. We explored the extension of this idea to include the mixed states.

We then encountered the question of quantifying entanglement. One can make entanglement monotones by utilizing concave functions on pure states and extending the definition to mixed states through the minimization over all pure state decompositions. Concurrence is an example of such an entanglement monotone. We also explored the properties of negativity as a separate measure of entanglement.

We then introduced the idea of k-separability that gives a hierarchy to classify different kinds of multipartite entanglement. We focused on the case of all-party entanglement, also known as genuinely multipartite entanglement. Finally, we introduced the all-party concurrence and showed that it is a proper measure of all-party entanglement.

In the rest of this thesis we focus on the multipartite entanglement among an arbitrary number of qubits. In the next chapter, we focus heavily on a special class of N-qubit states (X-states) and derive an algebraic formula to determine and quantify the all-party entanglement of such states. In chapter three we use this formula to explore the connection between the entanglement and purity in multiqubit systems. We also examine the idea of universality of X-states.

In the fourth chapter we sharpen our machinery for experimental explorations. We introduce a new measure of all-party entanglement and derive experimentally accessible bounds for its value. In the last chapter of this work we utilize the machinery we develop to study the dynamics of entanglement in different scenarii. We first study entanglement sudden death and finally study how the phenomenon of collapse and revival can be used to control the suppression and revival of the entanglement in

multipartite systems. Our analysis suggest a clear picture of the path that the system traverses in the Hilbert space.

Chapter 2

Theory of entanglement of N-qubit X-states

The problem of determining whether a two-qubit density matrice is entangled was first solved in the seminal work of Wootters [20]. The Wootters concurrence formula though effective is a prescription that involves calculating the eigenvalues of a matrix. Thus using concurrence formula in dynamical situations usually requires a numerical procedure, and this typically limits the feasibility of analytical investigations. Nevertheless, there are classes of states for which concurrence takes a very simple form. The simplest case is the case of a two-qubit pure state. A pure two-qubit state can always be written as

$$|\psi\rangle = \alpha|00\rangle + \beta|01\rangle + \gamma|10\rangle + \delta|11\rangle. \tag{2.0.1}$$

The concurrence of this state is $C(|\psi\rangle\langle\psi|) = 2\ |\alpha\delta - \beta\gamma|$. This formula, however, has a limited utility since in a dynamical scenario typically different systems couples with each other, or their environments, and do not remain pure. This is how the X-states were first propelled to the front of dynamical studies involving entanglement between two qubits. Their concurrence takes a simple form that can be used in analytical investigations and furthermore there are many dynamical scenarii in which the X-form of the state is robust. Their most famous appearance is the role they played in identification of the phenomenon of sudden death of entanglement by Yu and Eberly [51].

This chapter is devoted to introduction and examination of X-states. We first

discuss the two-qubit case and their properties and then discuss their extension to the case of many qubit density matrices. We then discuss how to find the many party entanglement for such states. We derive an algebraic formula for the all-party concurrence of such states. We finally discuss some of the subsets of X-states and their properties.

2.1 X-states: from two qubits to many qubits

It is always possible to write a density matrix of two qubits, $\hat{Q}$, as a sum of an X density matrix and a remaining matrix, that we call an O-matrix. Assume that the density matrix $\hat{Q}$, written in an orthonormal product basis $\{|00\rangle, |01\rangle, |10\rangle, |11\rangle\}$, reads:

$$\hat{Q} = \begin{pmatrix} Q_{11} & Q_{12} & Q_{13} & Q_{14} \\ Q_{21} & Q_{22} & Q_{23} & Q_{24} \\ Q_{31} & Q_{32} & Q_{33} & Q_{34} \\ Q_{41} & Q_{42} & Q_{43} & Q_{44} \end{pmatrix}. \tag{2.1.1}$$

Then $\hat{Q} = \hat{X} + \hat{O}$

$$= \begin{pmatrix} Q_{11} & 0 & 0 & Q_{14} \\ 0 & Q_{22} & Q_{23} & 0 \\ 0 & Q_{32} & Q_{33} & 0 \\ Q_{41} & 0 & 0 & Q_{44} \end{pmatrix} + \begin{pmatrix} 0 & Q_{12} & Q_{13} & 0 \\ Q_{21} & 0 & 0 & Q_{24} \\ Q_{31} & 0 & 0 & Q_{34} \\ 0 & Q_{42} & Q_{43} & 0 \end{pmatrix}. \tag{2.1.2}$$

The X matrix can be thought of as a density matrix itself, and so one can associate a concurrence to it. This concurrence takes a very simple form.

$$\begin{aligned} C(\hat{X}) &= \max\{0, |Q_{14}| - \sqrt{Q_{22}Q_{33}}, |Q_{23}| - \sqrt{Q_{11}Q_{44}}\} \\ &= \max\{0, C_1(\hat{X}), C_2(\hat{X})\}. \end{aligned} \tag{2.1.3}$$

The term X-matrix was first coined by Yu and Eberly [52, 51]. An X-state is a density matrix of two qubits, written in an orthonormal product basis, whose non-zero elements are only diagonal or anti-diagonal. The simple concurrence formula, given above is why these two-qubit states have been extensively used in studying the dynamics of entanglement between two qubits in many scenarii [53, 51, 54, 55, 56, 57, 58, 59]. Many of other properties of two-qubit X-states also take simple formulas too

[60].

As mentioned above the X-part of any two-qubit matrix is itself a density matrix. To see this note that positivity of $\hat{Q}$ ensures that $|Q_{23}| \leq \sqrt{Q_{22}Q_{33}}$, and $|Q_{14}| \leq \sqrt{Q_{11}Q_{44}}$. These two conditions ensure that eigenvalues of $\hat{Q}$ when projected on two subspaces $\{|01\rangle, |10\rangle\}$ and $\{|00\rangle, |11\rangle\}$ respectively, are non-negative. The matrix $\hat{X}$ is a convex sum of these two states and thus is positive itself. Furthermore $\hat{X}$ has a unity trace and is hermitian. These conditions guarantee that $\hat{X}$ is a density matrix itself. The question then arises whether there is a relation between the concurrence of any two-qubit density matrix and its X-part.

We will show that such a relation exists and in fact the concurrence of the X-part of any density matrix is smaller or equal to the concurrence of the whole matrix $C(\hat{Q}) \geq C(\hat{X})$. We will give two proofs for this statement, both we will later extend to X-states of many-qubit states, but one is especially important to help us find the all-party entanglement of N-qubit X-states.

In our first proof we show that for any $\hat{Q}$, the X-part of the density matrix $\hat{X}$ can be written as the result of a positive local map acting on $\hat{Q}$. Since the concurrence is a monotone of entanglement it should be, on average, non-increasing under such mapping and thus the concurrence of $\hat{X}$ shall be smaller than $C(\hat{Q})$. Let us call this mapping χ. One can show that for any two-qubit state

$$\chi(\hat{Q}) = \frac{1}{2}\left(\hat{Q} + (\hat{\sigma}_z \otimes \hat{\sigma}_z)\hat{Q}(\hat{\sigma}_z \otimes \hat{\sigma}_z)\right) = \hat{X}. \tag{2.1.4}$$

Our second proof is longer and admittedly more convoluted, but it gives the lower bound value explicitly with out the need to reference to the concurrence of an X-state. Thus an extension of it to the N qubits can be found to find a lower bound for the all-party concurrence of any qubits. We will use such an extension later in the coming section.

In the following we will prove that $C_1(\hat{X})$ is smaller or equal to the concurrence of the original matrix, $C(\hat{Q})$; i.e. $C_1(\hat{X}) \leq C(\hat{Q})$. The proof that $C_2(\hat{X}) \leq C(\hat{Q})$ is identical. Note that $C(\hat{X})$ is a basis-dependent quantity and our claim is that it is always smaller than or equal to the concurrence $C(\hat{Q})$ which is a basis-independent quantity. In addition, note that $\max\{0, C_1(\hat{X})\}$ is the concurrence of a density matrices for which the O-elements as well as Q_{23} and Q_{32} are put to zero. A similar remark can also made about $\max\{0, C_2(\hat{X})\}$. It will be shown that these ideas can also be generalized to the bipartite states of higher dimensions.

Let us first assume that $\hat{Q}$ is a pure state. For the pure state we defined in Eq.(2.0.1) we have

$$C_1(|\psi\rangle\langle\psi|) = 2\ |\alpha\delta| - 2\ |\beta\gamma|. \tag{2.1.5}$$

Using the triangle inequality returns the desired inequality

$$C(|\psi\rangle\langle\psi|) \geq |C_1(|\psi\rangle\langle\psi|)|. \tag{2.1.6}$$

We note that the basis that maximizes the $C_1(|\psi\rangle\langle\psi|)$ is the one for which $\gamma = \beta = 0$ which is equivalent to the Schmidt decomposition of the state. We now turn our attention to the case when $\hat{Q}$ is a mixed state. The concurrence of a mixed state is defined as

$$C(\hat{Q}) = \text{Min} \sum_i p_i\ C(|\psi_i\rangle\langle\psi_i|), \tag{2.1.7}$$

where the minimum is taken over all the pure decompositions of $\hat{Q}$:

$$\hat{Q} = \sum_i p_i\ |\psi_i\rangle\langle\psi_i|. \tag{2.1.8}$$

Let us assume that the decomposition that satisfies Eq.(2.1.7) reads

$$\hat{Q} = \sum_i P_i\ |\phi_i\rangle\langle\phi_i|, \tag{2.1.9}$$

$$C(\hat{Q}) = \sum_i P_i\ C(\hat{Q}^{(i)}), \tag{2.1.10}$$

where $\hat{Q}^{(i)} = |\phi_i\rangle\langle\phi_i|$. Since $|\phi_i\rangle$'s are pure states, we can use Eq. (2.1.6) and write

$$C(\hat{Q}) \geq \sum_i P_i\ C_1(\hat{Q}^{(i)}). \tag{2.1.11}$$

To complete our proof we seek to show that

$$\sum_i P_i\ C_1(\hat{Q}^{(i)}) \geq C_1(\hat{X}). \tag{2.1.12}$$

The explicit formulas for $C_1(\hat{Q}^{(i)})$ and $C_1(\hat{X})$, in terms of the elements of the $\hat{Q}^{(i)}$'s,

are

$$C_1(\hat{Q}^{(i)}) = 2(|Q_{14}^{(i)}| - \sqrt{Q_{22}^{(i)}Q_{33}^{(i)}}), \tag{2.1.13}$$

$$C_1(\hat{X}) = 2(|Q_{14}| - \sqrt{Q_{22}Q_{33}}), \tag{2.1.14}$$

where, for example, $Q_{14} = \sum_i P_i Q_{14}^{(i)}$. The following inequalities can be proved easily using the triangle and Cauchy-Schwarz inequalities:

$$\sum_i P_i |Q_{14}^{(i)}| \geq |\sum_i P_i Q_{14}^{(i)}| = |Q_{14}|, \tag{2.1.15}$$

$$\sum_i P_i \sqrt{Q_{22}^{(i)}Q_{33}^{(i)}} \leq \sqrt{\sum_i P_i Q_{22}^{(i)}} \sqrt{\sum_j P_j Q_{33}^{(j)}} = \sqrt{Q_{22}Q_{33}}\ .$$

By subtracting the above inequalities one can show that

$$\sum_i P_i\ C_1(\hat{Q}^{(i)}) \geq C_1(\hat{X}). \tag{2.1.16}$$

Two equations (2.1.11) and (2.1.16) complete our proof:

$$C(\hat{Q}) \geq C_1(\hat{X}). \tag{2.1.17}$$

Similarly one can show that $C(\hat{Q}) \geq C_2(\hat{X})$ and therefore

$$C(\hat{Q}) \geq \text{Max}\{0, C_1(\hat{X}), C_2(\hat{X})\} = C(\hat{X}), \tag{2.1.18}$$

which is the inequality that we sought to prove. That is, we have proved that if one ignores the O-elements of a density matrix, the concurrence of the remaining X matrix is always smaller than or equal to the concurrence of the original density matrix.

This inequality provides a sufficient condition that, if met, tells us that the state is entangled and gives a lower bound on its entanglement. For a density matrix that takes the X form, the inequality in Eq.(2.1.18) becomes an equality. However, the converse is not necessarily true, i.e., it is possible that the matrix $\hat{Q}$ does not have the X form in the basis in which it is presented, and yet the concurrence of the corresponding $\hat{X}$

is the same as for the original density matrix $\hat{Q}$. An example is given by

$$\frac{1}{2}|00\rangle + \frac{1}{\sqrt{3}}|01\rangle + \frac{1}{\sqrt{6}}|10\rangle + \frac{1}{2}|11\rangle. \tag{2.1.19}$$

The inequality that we derived above can be extended to the cases of bipartite states of higher dimension or even to the cases where we are concerned with more than two parties. We are going to discuss the multipartite case in detail and the bipartite case and the two-qubit cases can indeed be considered as special cases of that results. Thus here we only present the bipartite result.

There are different ways to generalize concurrence to higher dimensions [61, 43, 62]. We choose to work with the *I concurrence* that was first proposed by Rungta, et al. [43]. It was later shown to be an entanglement monotone [22]. Here we simply refer to *I concurrence* as concurrence as it is widely referred to in the literature. If we refer to the two parties of the system as A and B, the concurrence of a bipartite pure state is given by $\sqrt{2(1-\mathrm{Tr}[\hat{Q}_A^2])}$ where $\hat{Q}_A = \mathrm{Tr}_B[\hat{Q}]$ denotes the reduced density matrix of one of the subsystems. In analogy to the two-qubit case, we define

$$C_{ik,jl}(\hat{Q}) = 2\left(|Q_{ik,jl}| - \sqrt{Q_{il,il}Q_{jk,jk}}\right) \tag{2.1.20}$$

where, e.g., $Q_{ik,jl} = \langle i,k|\hat{Q}|j,l\rangle$. The quantity $C_{ik,jl}(\hat{Q})$ then plays the same role that previously $C_1(\hat{Q})$ played in the proof for the two qubit density matrices and similarly one can show that

$$C(\hat{Q}) \geq \mathrm{Max}\{0, C_{ik,jl}(\hat{Q}) \;\; (i \neq j, k \neq l)\}. \tag{2.1.21}$$

This is a sufficient condition for non-separability and the maximum of the $C_{ik,jl}$'s gives a lower bound for concurrence. The above lower bound can be thought of as a special case of a lower bound proposed for genuinely multipartite entanglement in [26] applied to a bipartite state.

2.2 The algebra of X-states

In the previous section we examined the properties of two-qubits X-states. In this section we focus on properties of such states in multiqubit systems. For two qubits the X-states are those states that, presented in a product orthonormal basis, have only

two-party coherences. This is equivalent to saying that the only non-zero elements of the density matrix are either diagonal or anti-diagonal. Conversely if we force the single party coherences of any two-qubit state, we are left with a proper density matrix. Such is not necessarily true for example for bipartite systems of higher dimension.

For the multiqubit case a similar idea can be drawn. Encountered with N qubits, one can have single party coherences, two party coherences, ..., and N-party coherences. Again a density matrix that, in a product orthonormal basis, has only N-party coherences is called an X-state. This is equivalent to having non-zero elements that are either diagonal or anti-diagonal. Furthermore, the converse is also true. For any matrix if one puts to zero all coherence elements, but the N-party coherences, one ends up with a valid density matrix. Below we examine some of the algebraic properties of such states and then prove that the connection with the two-qubit case is even deeper. We will prove that for any N-qubit density matrix the mapping that leads to the X-part is an LOCC map. Thus for any proper measure of entanglement, the value of the measure shall be smaller than the value of the same measure for the X-part of the same density matrix. Similarly to the case of two qubits we name the mapping that takes any density matrix to its X-part χ.

An algebraic characterization of X-states was presented in [63]. It is shown that any N-qubit X-state can be written in the following form:

$$X = \frac{1}{2^N} \sum_{i=0}^{2^N-1} \left(s_i \hat{S}_i + r_i \hat{R}_i \right), \tag{2.2.1}$$

where $s_0 = 1$, and s_i, r_i are real. To define $\hat{S}_i$ and $\hat{R}_i$, first note that any generator of SU(2^N) is a direct product of N generators of SU(2). $\hat{S}_i$ is the operator obtained by replacing, in the binary representation of i, 0's with $\hat{I}$ and 1's with $\hat{\sigma}_z$. $\hat{R}_i$ is the operator that is obtained similarly, but by replacing 0's with $\hat{\sigma}_x$ and 1's with $\hat{\sigma}_y$. For example,

$$\begin{aligned} \hat{S}_2 &= \hat{\mathbb{1}} \otimes \hat{\mathbb{1}} \otimes \cdots \otimes \hat{\sigma}_z \otimes \hat{\mathbb{1}} \\ \hat{R}_3 &= \underbrace{\hat{\sigma}_x \otimes \hat{\sigma}_x \otimes \cdots \otimes \hat{\sigma}_y \otimes \hat{\sigma}_y}_{N}. \end{aligned} \tag{2.2.2}$$

Let us define the sets $S = \bigcup_{i=0}^{2^N-1} \{\hat{S}_i\}$ and $R = \bigcup_{i=0}^{2^N-1} \{\hat{R}_i\}$. The set $S \cup R$ is closed under multiplication as well as commutation [63]. Furthermore, in S there are 2^{N-1}

operators whose commutation with every element of $S \cup R$ vanishes. These are elements of S with an even number of $\hat{\sigma}_z$'s in their multiplication. We name this subset C. Then the quantum operation χ, that takes any N-qubit density matrix and returns its X-part, is given by

$$\chi(\rho) = \frac{1}{2^{N-1}} \sum_{\hat{S}_i \in C} \hat{S}_i \rho \hat{S}_i^\dagger. \tag{2.2.3}$$

Below we prove that the mapping given in Eq. (2.2.3) returns the X-part of any density matrix. We do so by showing that every generator of SU(2^N), which is not in $S \cup R$ commutes with half of the elements of C and anticommutes with the other half. Since every N-qubit density matrix can be written as a linear sum of generators of SU(2^N), the coefficients of generators in $S \cup R$ survive the sum while the coefficients of the generators outside $S \cup R$ cancel out, leaving only the X-part of the density matrix. The special case of $N = 2$ is discussed in [64].

Let us first introduce two sets $\xi = \{\mathbb{1}, \hat{\sigma}_z\}$, $\eta = \{\hat{\sigma}_x, \hat{\sigma}_y\}$. Every generator of SU($2^N$) is given by a direct product of N operators from either η or ξ. We consider the arbitrary generator

$$\hat{\mathbf{A}} = \bigotimes_{j=1}^{N} \hat{a}_j \tag{2.2.4}$$

where $\hat{a}_j$ is either in ξ or η. We also choose an arbitrary element in C,

$$\hat{\mathbf{B}} = \bigotimes_{j=1}^{N} \hat{b}_j \tag{2.2.5}$$

where $\hat{b}_j$ is either $\hat{\sigma}_z$ or $\mathbb{1}$, and there are an even number of $\hat{b}_j$ for which $\hat{b}_j = \hat{\sigma}_z$. It is straightforward to show that the commutator has the form

$$\hat{\mathbf{A}}\hat{\mathbf{B}} \pm \hat{\mathbf{B}}\hat{\mathbf{A}} = (\bigotimes_{j=1}^{N} \hat{a}_j \hat{b}_j) \pm (\bigotimes_{j=1}^{N} \hat{b}_j \hat{a}_j). \tag{2.2.6}$$

We note that $\hat{b}_j \hat{a}_j = -\hat{a}_j \hat{b}_j$ only if $\hat{a}_j \in \eta$ and $\hat{b}_j = \hat{\sigma}_z$ and $\hat{b}_j \hat{a}_j = \hat{a}_j \hat{b}_j$ otherwise.

Consequently we find that

$$\hat{\mathbf{A}}\hat{\mathbf{B}} \pm \hat{\mathbf{B}}\hat{\mathbf{A}} = \hat{\mathbf{A}}\hat{\mathbf{B}}(1 \pm (-1)^q) \tag{2.2.7}$$

where q is the total number of times $\hat{a}_j \in \eta$ and $\hat{b}_j = \hat{\sigma}_z$. Thus $\hat{\mathbf{A}}$ and $\hat{\mathbf{B}}$ commute if q is even and they anti-commute otherwise. Therefore we need only count the number of operators in C for which q is even for an arbitrary operator $\hat{\mathbf{A}}$. This is simpler than it seems. Let us assume that there are a total of M $\hat{a}_j \in \eta$. The total number of ways an even number of $\hat{\sigma}_z$'s can be distributed among two sets, one of size M and one of size N-M, with an even number in each is given by

$$\sum_{i,j=0} \binom{M}{2i}\binom{N-M}{2j} = 2^{N-2}, \tag{2.2.8}$$

including the case of zero σ_z's which represents the identity. The set C has 2^{N-1} elements and thus $\hat{\mathbf{A}}$ anti-commutes with the other half of C. Note that this breaks if $M = 0$ or $N = 0$. But in that case $\hat{\mathbf{A}} \in S \cup R$ and all elements of C commute with $\hat{\mathbf{A}}$. This proves that Eq. (2.2.3) is an LOCC mapping.

It immediately follows that for any entanglement monotone, the entanglement of $\chi(\rho)$ is always smaller or equal to the entanglement of ρ. We will show that the lower bound of all-party concurrence that was derived in [26] can thus be understood as a special case of this inequality.

We note that the X-state can be defined completely different from their connection to X-states and through their algebraic symmetries. In principle one can also use other symmetries to define other classes of states, as is done in [63, 64]. Then one can define a hierarchy of inequalities for all entanglement monotones. The important step however is that as long as one cannot compute a measure of entanglement for such classes of states, not much is added in terms of our ability to study entanglement. In other words if we only knew that for some monotone of entanglement $E(\hat{\rho}) \geq E(\hat{X}_\rho)$ but we did not have the ability to compute $E(\hat{X}_\rho)$, such inequality would have very limited use. In the next section we address this problem and will derive an algebraic formula for the all-party concurrence of N-qubit X-states.

2.3 The all-party entanglement of X-states

In the previous section we study the algebraic properties of the X-states. In this section we study the all-party entanglement. The N-qubit version of the X-matrix [52] is a density matrix of N qubits, written in an orthonormal product basis, whose non-zero elements are only diagonal or anti-diagonal.

If the orthonormal basis for the X-matrix is $\{|0,0,\ldots,0\rangle, |0,0,\ldots,1\rangle, \ldots, |1,1,\ldots,1\rangle\}$, then one can always write an X-matrix in the form given below

$$\hat{X} = \begin{pmatrix} a_1 & & & & & & & z_1 \\ & a_2 & & & & & z_2 & \\ & & \ddots & & & \iddots & & \\ & & & a_n & z_n & & & \\ & & & z_n^* & b_n & & & \\ & & \iddots & & & \ddots & & \\ & z_2^* & & & & & b_2 & \\ z_1^* & & & & & & & b_1 \end{pmatrix}, \tag{2.3.1}$$

where $n = 2^{N-1}$, and we require $|z_i| \leq \sqrt{a_i b_i}$ and $\sum_i (a_i + b_i) = 1$ to ensure that $\hat{X}$ is positive and normalized. One can see why density matrices in this class are called X-matrices.

The concurrence of a two-qubit X-matrix takes a very simple form [52] and that is why these two-qubit states have been extensively used in studying the dynamics of entanglement between two qubits in many scenarii [52, 53, 51, 54, 55, 56, 57, 58, 59].

In the following we first derive a lower bound for the all-party concurrence of any X-states. For two-qubit states this lower bound reduces to the concurrence of the X-part of the density matrix. In light of this result one wonders whether this lower bound may be the exact value of the all-party concurrence even for many-qubit X-states. We will prove that this conjecture is correct.

In Ref. [26], Ma *et al.* presented a lower bound for the GM concurrence. The lower bound of GM concurrence, derived in Ref. [26], for an X-matrix is given by

$$C_{GM} \geq 2\max\{0, |z_i| - w_i\}, \ i = 0, 1, \ldots, n \tag{2.3.2}$$

where $w_i = \sum_{j\neq i}^{n} \sqrt{a_j b_j}$.

We will prove this relation for the case of three qubits. It includes all the essential elements that are needed to prove the general case and is more easily readable. The proof of the general case is given in [26]. Similarly to the two qubit case we first prove the inequality for a pure state. A three-qubit pure state can be written as

$$|\psi\rangle = a_0|000\rangle + a_1|001\rangle + a_2|010\rangle + a_3|011\rangle + a_4|100\rangle + a_5|101\rangle + a_6|110\rangle + a_7|111\rangle. \quad (2.3.3)$$

For three qubits we have only three bipartitions.

$$C_1^2 = 4|a_0a_7 - a_3a_4| + F_1$$
$$C_2^2 = 4|a_0a_7 - a_2a_5| + F_2$$
$$C_3^2 = 4|a_0a_7 - a_1a_6| + F_2$$

Where all F_i's are non-negative. Thus we can conclude that

$$C_1 \geq 2|a_0a_7| - 2|a_3a_4|$$
$$C_2 \geq 2|a_0a_7| - 2|a_2a_5|$$
$$C_3 \geq 2|a_0a_7| - 2|a_1a_6|$$

Thus we conclude

$$\begin{aligned} C_{GM} = \min\{C_1, C_2, C_3\} &\geq 2|a_0a_7| - 2(|a_3a_4| + |a_2a_5| + |a_1a_6|) \\ &= 2\rho_{17} - 2\sqrt{\rho_{11}\rho_{66}} - 2\sqrt{\rho_{22}\rho_{55}} - 2\sqrt{\rho_{33}\rho_{44}} \end{aligned}$$

Which is the result we wanted to prove. Note that the right hand side of the last equation is a concave function of the elements of the density matrix and thus similarly to the proof of the two-qubit case we can extend the inequality to mixed states too. This approach to derive inequalities is a prevalent technique that has been used in many of the results that deal with deriving inequalities whose violation signals entanglement [26, 25, 65]. Now we move to prove that the lower bound we derive above is the exact value of the all-party concurrence for N-qubit X-states.

In the following we will show that this lower bound is exact for all X-matrices. Without loss of generality we can assume that $\sqrt{a_1b_1} \geq \sqrt{a_ib_i}$. Since we have assumed that $\sqrt{a_1b_1} \geq \sqrt{a_ib_i}$, it is easy to show that $|z_i| - w_i \leq 0$ for $i > 1$, so that Eq. 2.3.2

reduces to

$$C_{GM}(X) \geq 2\max\{0, |z_1| - w_1\} \tag{2.3.4}$$

We will show that this bound is actually an equality. First let us prove a lemma that we will utilize in our proof.

Lemma: The GM concurrence of an X-matrix for which $a_1 b_1 \geq a_i b_i$, and $a_j = b_j = 0$ for all $j \neq \{i, 1\}$, is

$$C_{GM}(\hat{X}_{1i}) = 2\max\{0, |z_1| - \sqrt{a_i b_i}\} \tag{2.3.5}$$

Proof. We already know that this quantity is a lower bound of GM concurrence. Thus we only need to show that it is also an upper bound. We do this by mapping $\hat{X_{1i}}$ to a two-qubit density matrix, $\hat{R}$, and then show that $C_{GM}(\hat{X}_{1i})$ is bounded from above by Wootters's concurrence of $\hat{R}$, where $C(\hat{R}) = 2\max\{0, |z_1| - \sqrt{a_i b_i}\}$.

Before going forward let us introduce some notation. Since we are working with qubits, we can represent each vector (ket) of the above basis as a number from 0 to $2^N - 1$ written in the binary basis. For example, $|0, 0, \cdots, 0\rangle = |0\rangle$, $|0, \cdots, 0, 1\rangle = |1\rangle$, $|0, \cdots, 1, 0\rangle = |2\rangle$, and so on $|1, \cdots, 1, 1\rangle = |2^N - 1\rangle$. We also denote the bit-flipped states in the same way, $|\bar{i}\rangle = |2^N - i - 1\rangle$, for example, $|\bar{0}\rangle = |2^N - 1\rangle$. In places where we need to label the individual qubits, we do so by using a subscript on the bits.

We perform the mapping by focusing on a specific bipartition of the qubits. The four non-zero diagonal elements of $\hat{X}_{1i}$ are $\{a_1, a_i, b_1, b_i\}$, corresponding to projectors $\{|0\rangle\langle 0|, |i-1\rangle\langle i-1|, |\bar{0}\rangle\langle\bar{0}|,$ and $|\overline{i-1}\rangle\langle\overline{i-1}|\}$ respectively. Those qubits that contribute 1 to the ket $|i-1\rangle$ we designate as party F. The rest of the qubits we denote as party G. For example, with seven qubits, which we denote as $(q_1, q_2, q_3, q_4, q_5, q_6, q_7)$, where $i = 6$, the basis states are

$$\begin{aligned}
|0\rangle &= |0_1, 0_2, 0_3, 0_4, 0_5, 0_6, 0_7\rangle, \\
|5\rangle &= |0_1, 0_2, 0_3, 0_4, 1_5, 0_6, 1_7\rangle, \\
|127\rangle &= |1_1, 1_2, 1_3, 1_4, 1_5, 1_6, 1_7\rangle, \\
|122\rangle &= |1_1, 1_2, 1_3, 1_4, 0_5, 1_6, 0_7\rangle.
\end{aligned} \tag{2.3.6}$$

Then party F is given by qubits $(q_1, q_2, q_3, q_4, q_6)$, and the remaining two qubits, (q_5, q_7), make party G. Under this bipartition, we can write $\hat{X}_{1i}$ using the follow-

ing basis states,

$$|\downarrow_F\rangle = |0_1, 0_2, 0_3, 0_4, 0_6\rangle, \qquad |\uparrow_F\rangle = |1_1, 1_2, 1_3, 1_4, 1_6\rangle,$$
$$|\downarrow_G\rangle = |0_5, 0_7\rangle, \qquad |\uparrow_G\rangle = |1_5, 1_7\rangle,$$

$$\begin{aligned}\hat{X}_{1i} = {} & a_1|\downarrow_F\downarrow_G\rangle\langle\downarrow_F\downarrow_G| + b_1|\uparrow_F\uparrow_G\rangle\langle\uparrow_F\uparrow_G| \\ & + a_i|\downarrow_F\uparrow_G\rangle\langle\downarrow_F\uparrow_G| + b_i|\uparrow_F\downarrow_G\rangle\langle\uparrow_F\downarrow_G| \\ & + z_1|\downarrow_F\downarrow_G\rangle\langle\uparrow_F\uparrow_G| + z_1^*|\uparrow_F\uparrow_G\rangle\langle\downarrow_F\downarrow_G| \\ & + z_i|\downarrow_F\uparrow_G\rangle\langle\uparrow_F\downarrow_G| + z_i^*|\uparrow_F\downarrow_G\rangle\langle\downarrow_F\uparrow_G|, \end{aligned} \tag{2.3.7}$$

We see that if we restrict attention to the subspace defined by the non-zero elements of $\hat{X}_{1i}$ we can map $\hat{X}_{1i}$ to a two qubit density matrix, $\hat{R}$, which, in the basis $\{|\downarrow_F\downarrow_G\rangle, |\downarrow_F\uparrow_G\rangle, |\uparrow_F\downarrow_G\rangle, |\uparrow_F\uparrow_G\rangle\}$, reads

$$\hat{X}_{1i} \longrightarrow \hat{R} = \begin{pmatrix} a_1 & & & z_1 \\ & a_i & z_i & \\ & z_i^* & b_i & \\ z_1^* & & & b_1 \end{pmatrix}. \tag{2.3.8}$$

Now that we have a two-qubit density matrix, we can take advantage of Wootters's concurrence. Note that from each pure-state decomposition (PSD) of $\hat{R}$ one can make a PSD of $\hat{X}_{1i}$ by mapping the basis states of the two-qubit system back to the multi-qubit basis states. We pick the PSD whose average concurrence is the minimum among all possible PSD's of $\hat{R}$. Thus

$$\hat{R} = \sum_i p_i|\psi_i\rangle\langle\psi_i|, \quad C(\hat{R}) = \sum_i p_i C(|\psi_i\rangle). \tag{2.3.9}$$

In Eq. 2.3.9, $C(\hat{R})$ is Wootters's concurrence, which, by definition, is equal to the minimum average concurrence over all possible PSD's of $\hat{R}$. As mentioned before, each pure state $|\psi_i\rangle$ can be mapped back to an N-qubit state ($|\psi_i\rangle \to |\Psi_i\rangle$), producing a PSD for $\hat{X}_{1i}$,

$$\hat{X}_{1i} = \sum_i p_i|\Psi_i\rangle\langle\Psi_i|. \tag{2.3.10}$$

Since GM concurrence is convex by definition, we have

$$C_{GM}(\hat{X}_{1i}) \leq \sum_i p_i C_{GM}(|\Psi_i\rangle). \tag{2.3.11}$$

For a pure state the GM concurrence is defined by

$$C_{GM}(|\Psi_i\rangle) = \min_j \sqrt{2}\sqrt{1 - \Pi_j(|\Psi_i\rangle)}, \tag{2.3.12}$$

where the minimum is taken over all bipartitions, J, of the N qubits. Therefore, the GM concurrence must be bounded by any specific bipartition, including the bipartition of the N qubits to party F and party G.

$$C_{GM}(|\Psi_i\rangle) \leq \sqrt{2}\sqrt{1 - \Pi_{F|G}(|\Psi_i\rangle)}. \tag{2.3.13}$$

Using the same mapping as for Eq. 2.3.8 it is easy to show that $C(|\psi_i\rangle)$ is equal to the right hand side of Eq. 2.3.13. Note that $|\psi_i\rangle\langle\psi_i|$ and $|\Psi_i\rangle\langle\Psi_i|$ are the same density matrices. We have only renamed (and not changed) the bases vectors and that does not change any of the reduced density matrices. Therefore we conclude that

$$\begin{aligned} C_{GM}(\hat{X}_{1i}) &\leq \sum_i p_i C_{GM}(|\Psi_i\rangle) \leq \sum_i p_i C(|\psi_i\rangle) \\ &= C(\hat{R}) = 2\max\{0, |z_1| - \sqrt{a_i b_i}\}, \end{aligned} \tag{2.3.14}$$

where the right most equality is found by evaluating Wootters's concurrence for $\hat{R}$ under the assumption $a_1 b_1 \geq a_i b_i$. This upper bound matches the lower bound and therefore it is the exact value of $C_{GM}(\hat{X}_{1i})$. □

Next, we generalize this result to all the X-matrices. We do so by decomposing the X-matrix into a convex sum of $\hat{X}_{1i}$ matrices. Let us first look at the case for which $|z_1| - w_1 \geq 0$.

(a) $|z_1| - w_1 \geq 0$. Note that $|z_i| - w_i \leq 0$ for $i \geq 2$ since $\sqrt{a_1 b_1} \geq \sqrt{a_i b_i} \geq |z_i|$. First by a change of phase of the basis, which is a local unitary transformation, we change z_1 to $|z_1|$. This only changes the phase of the other off-diagonal elements. Then we

decompose $\hat{X}$ in the following form.

$$\hat{X} = \hat{A} + \sum_{i>1}^{n} \hat{S}_i, \tag{2.3.15}$$

where $\hat{S}_i$ is an $\hat{X}_{1i}$ matrix whose two-qubit counterpart reads

$$\hat{R}_i = \begin{pmatrix} x_i & & & \sqrt{a_i b_i} \\ & a_i & z_i & \\ & z_i^* & b_i & \\ \sqrt{a_i b_i} & & & y_i \end{pmatrix}, \tag{2.3.16}$$

where

$$\begin{aligned} A_{11} &= a_1(1 - \frac{w_1}{\sqrt{a_1 b_1}}), \quad A_{2n,2n} = b_1(1 - \frac{w_1}{\sqrt{a_1 b_1}}), \\ A_{1,2n} &= A_{2n,1} = |z_1| - w_1, \\ A_{i,j} &= 0 \quad i \neq \{1, 2n\}, \text{or} \quad j \neq \{1, 2n\}, \\ x_i &= \frac{a_1\sqrt{a_i b_i}}{w_1}, \qquad y_i = \frac{b_1\sqrt{a_i b_i}}{w_1}. \end{aligned} \tag{2.3.17}$$

It can be shown that $\hat{S}_i$'s are all proportional to valid density matrices, since they are non-negative hermitian matrices. The proportionality constant is between zero and one and can be interpreted as probability. Using the above lemma one can show that all $\hat{S}_i$'s are biseparable matrices (though not normalized). Regarding the first matrix in the decomposition, the proportionality constant is $A_{11} + A_{2n,2n}$, and its GM concurrence is $2(|z_1| - w_1)/(A_{11} + A_{2n,2n})$. Due to the convexity of GM concurrence we conclude that

$$(A_{11} + A_{2n,2n})\frac{2(|z_1| - w_1)}{A_{11} + A_{2n,2n}} = 2(|z_1| - w_1) \tag{2.3.18}$$

is an upper bound for the GM concurrence of $\hat{X}$. Since $2(|z_1| - w_1)$ is also a lower bound for the concurrence, it is the exact value of the GM concurrence.

Note that for the above decomposition to work we had to assume that $|z_1| \geq w_1$. We now turn to the case $|z_1| < w_1$. We seek to show that all such density matrices are biseparable. We consider two different scenarios.

(b) $\sqrt{a_1 b_1} \geq w_1$. In this case the matrix $\hat{X}$ can be decomposed to matrices similar

to the previous case.

$$\hat{X} = \sum_{i>1}^{n} \hat{S}'_i, \tag{2.3.19}$$

where $\hat{S}'_i$ is an $\hat{X_{1i}}$ matrix whose two-qubit counterpart reads

$$\hat{R}'_i = \begin{pmatrix} a_1T_i & & & z_1T_i \\ & a_i & z_i & \\ & z_i^* & b_i & \\ z_1^*T_i & & & b_1T_i \end{pmatrix}, \quad T_i = \frac{\sqrt{a_ib_i}}{w_1}. \tag{2.3.20}$$

Since $|z_1|T_i \leq \sqrt{a_ib_i}$ and $|z_i| \leq \sqrt{a_1b_1}T_i$, we can invoke Lemma 1 to confirm $\hat{R}'_i$ is biseparable for all i. The fact that $\hat{R}'_i$ is not normalized does not interfere with the proof of biseparability as one can always factor out $\mathrm{Tr}[\hat{R}'_i]$. Now we focus on the last case.

(c) $\sqrt{a_1b_1} < w_1$. In this case we divide our matrix into two positive semi-definite matrices $\hat{X} = \hat{K}_1(t,r) + \hat{K}_1(r,t)$.

$$\hat{K_1}(t,r) = \begin{pmatrix} a_1t & & & & & & z_1t \\ & a_2r & & & & z_2r & \\ & & \ddots & & \iddots & & \\ & & & a_nr & z_nr & & \\ & & & z_n^*r & b_nr & & \\ & & \iddots & & \ddots & & \\ & z_2^*r & & & & b_2r & \\ z_1^*t & & & & & & b_1t \end{pmatrix},$$

where

$$t = \frac{w_1}{w_1 + \sqrt{a_1b_1}}, \quad \text{and} \quad r = 1 - t.$$

Note that since $w_1 \leq 3\sqrt{a_1b_1}$, then $\frac{3}{4} \geq t > r$. One can show that

$$t\sqrt{a_1b_1} = rw_1, \tag{2.3.21}$$

which guarantees that $\hat{K}_1(t,r)$ falls in the category of case (a). Since

$$\begin{aligned} t|z_1| &\leq rw_1, \\ r|z_j| &\leq (t-r)\sqrt{a_1 b_1} + rw_j, \end{aligned} \tag{2.3.22}$$

$\hat{K}_1(t,r)$ is biseparable. Regarding matrix $\hat{K}_1(r,t)$, since

$$\begin{aligned} r|z_1| &\leq tw_1, \\ t|z_j| &\leq r\sqrt{a_1 b_1} + t\sum_{i\neq 1,j}^{n} \sqrt{a_i b_i}, \end{aligned} \tag{2.3.23}$$

it does not fall in the category of case (a) and thus belongs to either case (b) or case (c). If it falls in the category of case (b) then we can conclude that it is biseparable. If not, we divide $\hat{K}_1(t,r)$ into two matrices $\hat{K}_1(t,r) = \hat{K}_2(t',r') + \hat{K}_2(r',t')$, as before. Each time we divide a matrix in this way the trace of the remaining part is strictly smaller than the trace of the step before: $\mathrm{Tr}[\hat{K}_i(r^i,t^i)] \leq \left(\frac{3}{4}\right)^i$. Thus, we can write the matrix $\hat{X}$ as a convex sum of biseparable states and a remaining part that can be made arbitrarily close to zero. Therefore matrix $\hat{X}$ is a biseparable matrix. This completes the proof for all X-matrices. Therefore, we have proved that the GM concurrence of a N-qubit X-matrix is

$$C_{GM}(\hat{X}) = 2\max\{0, |z_i| - w_i\}, \quad 1 \leq i \leq n \tag{2.3.24}$$

2.3.1 GHZ-diagonal states

Before closing this section we introduce an important subclass of X-states, namely the GHZ-diagonal states. GHZ states provide a complete basis for the Hilbert space. A class of states that can be directly linked to GHZ-states are the state that can be written as a convex sum of GHZ states, hence the name GHZ-diagonal states. In terms of X-states a GHZ-diagonal state takes a very simple form. Each GHZ state is an equally weighted coherent superposition of two spin flipped product states. For each GHZ state, there exists a GHZ state of the same spin flipped states but with the opposite sign between the two product states. Any convex sum of the density matrices of these two density matrices will have equal diagonal terms for the product states. One can show that the converse is also true. Any X state with the condition of $a_i = b_i$ can be shown to be a convex sum of GHZ-states. In the coming chapters

we will examine the entanglement properties of these states more carefully and derive a set of experimentally accessible bounds that are especially useful for states that are close to GHZ-diagonal states.

2.4 Chapter summary

N-partite entanglement, either as a resource for quantum computation or as a fundamental property of quantum theory, has been difficult to quantify, especially for mixed states. This is an important drawback since many of the algorithms in quantum computation need N-partite entanglement between a large number of qubits, and inevitable interaction of these qubits with the environment renders initial pure states mixed and diminishes their entanglement. Thus it is of interest to understand, quantitatively, the dynamics of N-partite entanglement when the qubits sharing it come in contact with different environments. In this chapter, we have found an algebraic formula for the genuinely N-partite (all-party) concurrence of N-qubit density matrices that can be written as X-matrices in an orthonormal product basis.

We first reviewed two-qubit X-states and discussed some of its entanglement properties, most importantly the relation between the concurrence of the entanglement of the X-part of any density matrix with the concurrence of the whole matrix. We then generalized the X-states to include the case of N qubits. We proved that for any proper measure of entanglement the entanglement of the X part of the density matrix is smaller than than entanglement of the whole matrix. We proved this result by showing that the mapping from the whole matrix to its X part is a LOCC mapping. Finally we focused on the X-states and derived an algebraic formula for the all-party concurrence of all such matrices. To achieve this we used the previously derived lower bound of the all-party concurrence and showed that we can always find a pure state decomposition whose average all-party concurrence matches the value of the lower bound. Thus such a decomposition is the optimal pure state decomposition and the lower bound is the actual value of the all-party concurrence.

The developments we laid out in this chapter allows N-partite entanglement to be quantified for X states. The formula opens up the possibility of studying entanglement dynamics of N-qubit states in different scenarii, as long as the X-form of the density matrix is preserved. In the following chapters we are going to use this result in three different ways. First we explore the connection between the all-party entanglement and mixedness in the next chapter. We then use our result to derive bounds that

are more experimentally accessible in chapter five, and finally we use the available machinery to study the entanglement dynamics in multiqubit open systems,

Chapter 3

Maximally entangled mixed X-states

In the previous chapter we studied the all-party entanglement for multiqubit states. We derived an algebraic formula for the all-party concurrence of all such states. In this chapter we take advantage of this formula to explore the Hilbert space of multiqubit states. The main question that we lightly entertain here regards the idea of universality. By universality we mean that a class of states can achieve all possible values of a set of quantities. Thus if a quantity is a resource then we only need to create/explore the universal subset and not all of the Hilbert space.

In the first section of this chapter we discuss and explore the idea of universality for two-qubit states. For the pair of concurrence-linear entropy, the two-qubit X-states are universal, and we discuss other universal properties of two-qubit X-states. In the next section we explore a similar idea of universality for N-qubit X-states. For this set we find the X-states that for a given value of linear entropy are maximally entangled. Examination of such states gives us some evidence that such states may be maximally entangled mixed states for all N-qubit X-states. We finish the chapter with a discussion on what is more to be done on this subject.

3.1 The universality of two-qubit X-states

The question regarding the maximally entangled states was first raised by Ishizaka and Hiroshima [66]. They introduced a class of two-qubit states whose entanglement of formation does not increase under any unitary transformation. They proved their

result for matrices with ranks smaller than four. For two-qubit states of rank four the result was confirmed numerically. They also examined that their observation also holds for negativity which is also a measure of two-qubit entanglement.

The question was then picked up in a separate paper [67]. where the class of two-qubit maximally entangled states was derived directly. The maximally entangled states are defined through the following observation. The set of pure states includes the Bell states that are the maximally entangled states. The set of completely mixed states, on the other hand, only includes separable states. One then wonders for the subset of states of a given degree of mixedness (or purity), what is the maximum value of entanglement.

There are a number of measures for the degree of purity. One can use either purity $\mathrm{Tr}[\hat{\rho}^2]$, or the von Neumann entropy, given by $-\mathrm{Tr}[\hat{\rho}\ln\hat{\rho}]$. We use the linear entropy which is defined by

$$S = \frac{d}{d-1}(1 - \mathrm{Tr}[\hat{\rho}^2]) \tag{3.1.1}$$

where d is the dimensionality of the density matrix. The linear entropy ranges from 0 to 1 with 0 indicating the density matrix to be a pure state and 1 indicating $\hat{\rho}$ to be completely mixed.

The authors proposed an ansatz based on the intuition that among non-diagonal elements, the two-party coherences are more directly related to the entanglement as opposed to single party coherences. Among the class of ansatz the authors found the class of states that are maximally entangled for a given linear entropy. These states are

$$\hat{\rho}_{MEMS} = \begin{pmatrix} g(\gamma) & 0 & 0 & \gamma/2 \\ 0 & 1-2g(\gamma) & 0 & 0 \\ 0 & 0 & 0 & 0 \\ \gamma/2 & 0 & 0 & g(\gamma) \end{pmatrix}, \quad g(\gamma) = \begin{cases} 1/3 & \gamma < 2/3, \\ \gamma/2 & \gamma \geq 2/3. \end{cases} \tag{3.1.2}$$

The concurrence of these states is γ, and their linear entropy is given by [67]

$$S = \frac{2}{3}[4g(\gamma)(2-3g(\gamma)) - \gamma^2] \tag{3.1.3}$$

In Fig. (3.3) we plot the concurrence versus linear entropy for 10^6 randomly, and uniformly chosen two-qubit states. The red line represents the set of maximally en-

tangled states (MEMS). As expected no point lays beyond the red line boundary confirming the fact that such states are indeed MEMS for concurrence versus linear entropy. The similar plot in reference [67] plot the tangle versus the linear entropy but since tangle, linear entropy and concurrence are directly related for two qubit states, we expect the same MEMS for all three quantities.

Another approach to the problem was developed by Verstraete, *et al.* [68]. They asked for a given two qubit density matrix what is the unitary transformation that leads the maximal entanglement. It was shown in [68] that for two qubit states the answer is given by the following theorem.

for the density matrix $\hat{\rho} = \Phi\Gamma\Phi^{\dagger}$ and the eigenvalues $\{\lambda_i\}$ that are sorted in the nonascending order, the entanglement of formation (and thus concurrence) is maximized if and only if the global transformation is of the form

$$U = (U_1 \otimes U_2) \begin{pmatrix} 0 & 0 & 0 & 1 \\ \frac{1}{\sqrt{2}} & 0 & \frac{1}{\sqrt{2}} & 0 \\ \frac{1}{\sqrt{2}} & 0 & \frac{-1}{\sqrt{2}} & 0 \\ 0 & 1 & 0 & 0 \end{pmatrix} D_{\phi}\Phi^{\dagger} \tag{3.1.4}$$

where D_ϕ is a diagonal unitary matrix. The resulting concurrence $\hat{\rho}' = U\hat{\rho}U^{\dagger}$ is then given by

$$C = \max\{0, \lambda_1 - \lambda_3 - 2\sqrt{\lambda_2\lambda_4}\} \tag{3.1.5}$$

Verstraete, *et al.* [68] also showed that the same transformation also maximizes the negativity as well as relative entropy of entanglement.

We finish this section by commenting on two recent efforts in regard the question of universality. First we comment on the recent work by Hedeman who has presented numerical evidence that two-qubit X-states are universal [69]. The other study is the work of Mendonça, *et al.* [70] that have proven that two-qubit X-states are indeed universal. Here by universality we mean that for any pair of concurrence and entropy that can be achieved by a physical state the same pair can be achieved by an X state. In fact the universality goes further and work for any pair of concurrence and a spectrum of density matrix.

In a recent attempt at the problem of universality of two-qubit X-states, Hedemann [69] has presented strong numerical evidence that in the plane of concurrence-purity, the X-states are universal. To show this, Hedemann focused on the idea of entangle-

ment preserving unitary (EPU) transformations. These are unitary transformations that preserve the value of a measure of entanglement. An obvious example of such transformations are the local unitary transformations, i.e. any proper of measure of entanglement is preserved under all local unitary transformations. Then numerical evidence was presented supporting the idea that any state can be transformed to an X-state through an EPU transformation. Since the spectrum and thus the purity are invariant under all unitary transformation this evidence is equivalent to evidence for the universality of X-states.

More recently and in a separate note, Mendonça, *et al.* [70], proved that indeed two-qubit X-states are universal. To prove this result the authors used the unitary entanglement maximizing transformation that was developed by Verstraete, *et al.* [68]. This transformation leads to an X-state of the same spectrum and entropy and equal or higher entanglement than the initial density matrix. In the last step the authors prove that this matrix can always be disentangled via a unitary transformation that preserves the X-form of the density matrix. Thus we can disentangle via such a transformation until the value of the measure of entanglement becomes the same as the value of the measure for the original state. Thus for any density matrix of a given spectrum, and purity and a given entanglement, we can find an X-state that has the same spectrum and purity and the same entanglement. This confirms that two-qubit X-states are universal. Note that the above result implies universality for all different measures of entanglement and not only for concurrence.

An immediate question to this section regards the universality of multiqubit X-states. Currently this is an open question. In the following section we will find the maximally entangled mixed states among N-qubit X-states. We will show that they have the same form as the MEMS for all two-qubit X-states. This similarity is consistent with the conjecture that even for N qubits, X-states may be universal.

3.2 What are MEMS for N qubits?

In the previous section we discussed the idea of universality of X-states and some of its different implications for two-qubit X-states. Moving beyond the simplest case of two qubits similar questions arise naturally. Are N-qubit X-states universal? What are the maximally entangled mixed states for a given linear entropy for N qubits. In this section we find the maximally entangled mixed states among the X-states. We find the class of X-states that for a given linear entropy have the maximum possible

all-party concurrence. We call this class of states XMEMS. For two qubits XMEMS matches the two-qubit MEMS. We also find the critical amount entropy, as a function of N, above which no X-states possesses all-party entanglement. We will prove that the critical entropy is given by

$$S_{cr}(N) = \frac{2^{2N-1}}{(2^N-1)(2N-1)+1}. \tag{3.2.1}$$

The critical entropy increases as a function of N. This means that for large N it is possible to find highly mixed states that possess genuinely N-partite entanglement.

3.2.1 numerical exploration

We first explore the idea of maximally entangled X-states numerically. We produce 10^6 random three qubit X-states. We then calculate both the linear entropy and all-party concurrence for each of the states and plot them. We make two qualitative observation from the plot. First is that as the linear entropy increases the maximum achievable all-party entanglement decreases. The second observation regards the critical entropy, that beyond a critical entropy no state possesses entanglement. Such observation can be made explicitly quantitative if we find the class of states that lie on the boundary of the entanglement-entropy plane. As mentioned, we will refer to this class of states as maximally entangled mixed X-states and denote them with XMEMS. We aim to determine XMEMS analytically in this section.

3.2.2 Maximally entangled mixed X-states

We use the same parametrization for X-states that we utilized in the previous chapter. Without loss of generality, we assume that $|z_1| \geq |z_i|$ for all i's. Thus the all-party concurrence is given by $C(X) = 2(|z_1| - w_1)$. Remember that $w_1 = \sum_{j\neq 1}^{2^{N-1}} \sqrt{a_j b_j}$. In the following we propose a mapping that takes any X state to a state $\bar{X}$ that has the same all-party concurrence but a higher linear entropy.

The mapping is defined through the elements of $\bar{X}$ that are given by the following

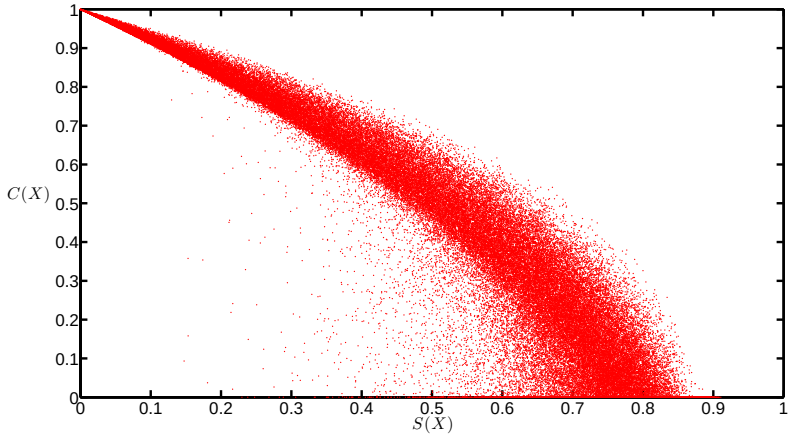

Figure 3.1: All-party concurrence and linear entropy plane for three-qubit X-states. Each of the points corresponds to the all-party concurrence and entropy of a randomly generated X-state. We are interested in the states that make the boundary as well as the critical entropy.

relations.

$$\bar{a}_1 = a_1 \tag{3.2.2}$$

$$\bar{a}_i = a_i + b_i, \qquad i > 1 \tag{3.2.3}$$

$$\bar{b}_1 = b_1 \tag{3.2.4}$$

$$\bar{b}_i = \bar{z}_i = 0, \qquad i > 1 \tag{3.2.5}$$

$$\bar{z}_1 = |z_1| = w_1. \tag{3.2.6}$$

One can readily check that the trace of $\bar{X}$ remains 1, and our mapping from X to $\bar{X}$ is positive. Furthermore the all-party concurrence is conserved under this mapping:

$$C(X) = C(\bar{X}) \tag{3.2.7}$$

Next we will show that the linear entropy is increasing under our mapping, i.e. the entropy of $\bar{X}$ is equal or more than the linear entropy of X. To show this we subtract the linear entropy of the two matrices.

$$S(\bar{X}) - S(X) = \left(\frac{2^{N+1}}{2^N - 1}\right) \times \sum_{i\neq 1}^{n} \left(|z_i|^2 + 2\sqrt{a_i b_i}(|z_1| - w_1)\right) \geq 0 \tag{3.2.8}$$

Note that our assumption that X is an entangled state implies that $|z_1| \geq \sum_{i\neq 1}^{n} \sqrt{a_i b_i}$.

The facts that the above mapping conserves the all-party concurrence and increases the linear entropy implies that the maximally entangled mixed states have to be conserved under such mapping and thus possess a similar form to $\bar{X}$ for which all the lower diagonal elements except $\bar{b}_1$ vanish.

Let us introduce a slight change of notation, and parameterize the XMEMS in the following form.

$$\hat{X} = \begin{pmatrix} \alpha+|\gamma| & & & & & & \gamma \\ & \bar{a}_2 & & & & 0 & \\ & & \ddots & & \iddots & & \\ & & & \bar{a}_n & 0 & & \\ & & & 0 & 0 & & \\ & & \iddots & & \ddots & & \\ & 0 & & & & 0 & \\ \gamma^* & & & & & & \beta+|\gamma| \end{pmatrix}, \tag{3.2.9}$$

To ensure the positivity and a unity trace, we also require

$$\alpha + |\gamma| \geq 0 \tag{3.2.10}$$

$$\beta + |\gamma| \geq 0 \tag{3.2.11}$$

$$\alpha\beta + (\alpha+\beta)|\gamma| \geq 0 \tag{3.2.12}$$

$$\alpha + \beta + 2|\gamma| + \sum_{i=2}^{n} \bar{a}_i = 1 \tag{3.2.13}$$

This parametrization is inspired by a similar parametrization in [67]. The all-party concurrence of such a state is given by $2|\gamma|$. Now we need to find that given γ for what values of the parameters maximize the entropy. This is equivalent to keeping the off-diagonal elements constant. Keeping the off-diagonal element constant, entropy or mixedness is maximized if all the possible diagonal elements are equally populated:

$$\alpha = \beta = x, \tag{3.2.14}$$

$$\bar{a}_2 = \bar{a}_3 = \cdots = \bar{a}_n = y, \tag{3.2.15}$$

where we have defined two new variables, x, y. Using the constraint of trace unity, we

can eliminate y in favor of x and rewrite the entropy of the density matrix as:

$$S(\bar{X}) = \frac{2^N}{2^N - 1}\left(A(x + |\gamma|)^2 + B(x + |\gamma|) + c\right) \tag{3.2.16}$$

where

$$A = -2\left(\frac{n+1}{n-1}\right), \tag{3.2.17}$$

$$B = \frac{4}{n-1}, \tag{3.2.18}$$

$$C = \left(1 - \frac{1}{n-1} - 2|\gamma|^2\right). \tag{3.2.19}$$

We now need to maximize the linear entropy, $S(\bar{X})$, for a given value of γ. We also need to make sure that the constraints of positivity are met. Thus $x, y \geq 0$ and $2(x + |\gamma|) + (n-1)y = 1$. This last equation implies $(x + |\gamma|) \leq 1/2$. Keeping these constraints in mind, we plot $S(\bar{X})$ in Fig. [FIGURE] as a function of $x + |\gamma|$. We note that when $|\gamma| \leq 1/(n+1)$ the maximum of $S(\bar{X})$ occurs at $x + |\gamma| = 1/(n+1)$ and $y = 1/(n+1)$. On the other hand, when $(x + |\gamma|) \geq 1/2$, the maximum occurs when $x = 0$, and $y = (1 - 2|\gamma|)/(n-1)$. With these considerations, we finally get the following form of the maximally entangled mixed X-states.

$$\hat{X}_{MEMS} = \begin{pmatrix} f(\gamma) & & & & & & & \gamma \\ & g(\gamma) & & & & & 0 & \\ & & \ddots & & & \iddots & & \\ & & & g(\gamma) & 0 & & & \\ & & & 0 & 0 & & & \\ & & \iddots & & & \ddots & & \\ & 0 & & & & & 0 & \\ \gamma^* & & & & & & & f(\gamma) \end{pmatrix}, \tag{3.2.20}$$

where

$$f(\gamma) = \begin{cases} \frac{1}{n+1} & 0 \leq |\gamma| \frac{1}{n+1} \\ |\gamma| & \frac{1}{n+1} \leq |\gamma| \leq \frac{1}{2} \end{cases} \tag{3.2.21}$$

and

$$g(\gamma) = \begin{cases} \frac{1}{n+1} & 0 \leq |\gamma| \frac{1}{n+1} \\ \frac{1-2|\gamma|}{n-1} & \frac{1}{n+1} \leq |\gamma| \leq \frac{1}{2} \end{cases} \tag{3.2.22}$$

As noted earlier these are the states that also have the maximum entanglement for a given value of entropy. The degree of all-party entanglement is $2|\gamma|$ and the linear entropy is given by

$$S(X_{MEMS}) = \frac{2^N}{2^N - 1} \left(A f(\gamma)^2 + B f(\gamma) + c \right). \tag{3.2.23}$$

In fig. 3.2 we plot the entanglement versus entropy for a million different matrices. We pick a XMEMS and add to it a random X-state and calculate the entanglement and the entropy. This allows the boundary in the entanglement-entropy plane explicitly. In a clear agreement with the analytical result we see that no randomly generated point violate the boundary. We note that the general results derived here reduces

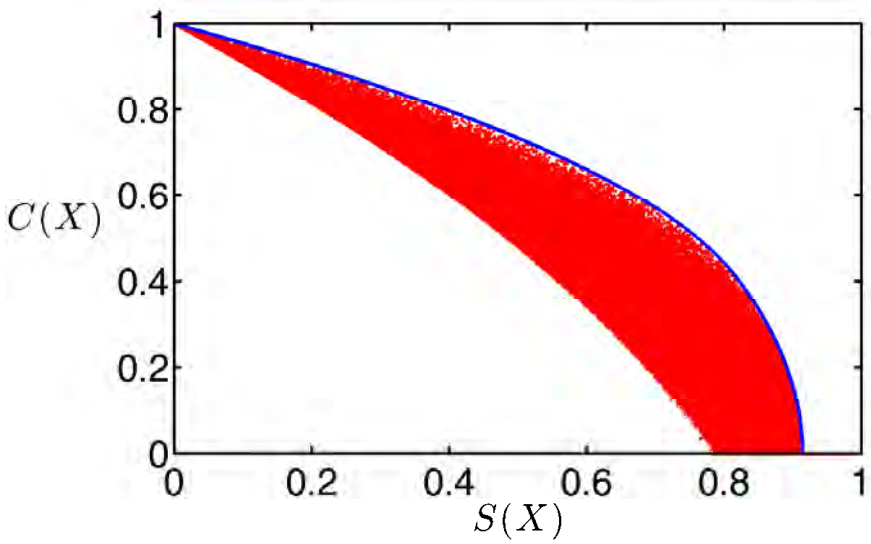

Figure 3.2: Entanglement and entropy of randomly generated three-qubit X-states. The solid line corresponds to the XMEMS for three qubits. We see that all the points lie inside the solid line, as we expect from our analytical solution.

correctly to the results derived by Munro *et al.* for $N = 2$ [67]. We reiterate that analysis here is restricted to the X-states whereas the analysis in the previous work includes all two-qubit density matrices.

Letting $\gamma = 0$, we also find the critical entropy above which no X-state possesses entanglement. This critical entropy as a function of N is given by

$$S_{cr}(N) = \frac{2^{2N-1}}{(2^N - 1)(2N - 1) + 1}. \tag{3.2.24}$$

For $N = 2$ this critical entropy is $8/9$. In Fig. 3.3 we plot this critical entropy as a function of N. We see that the critical entropy is an increasing function of N and it approaches unity asymptotically. This implied that as N increases, we can have states that are more mixed and still exhibit all-party entanglement.

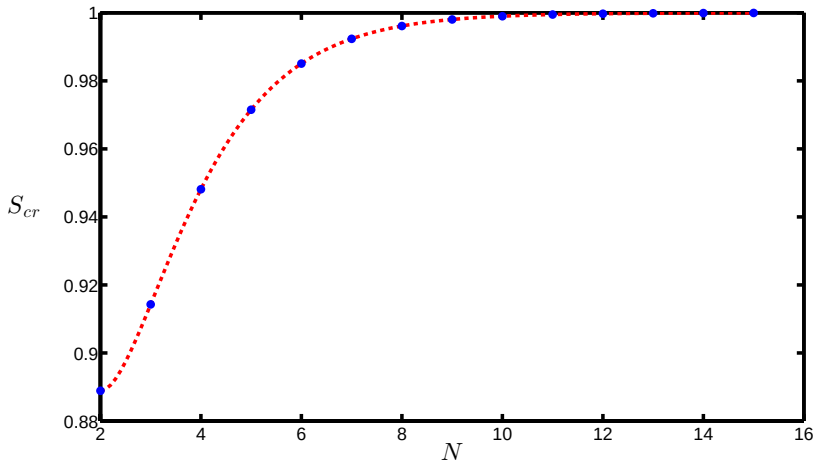

Figure 3.3: Critical entropy, S_{cr}, as a function of the number of participating qubits, N. Note that the critical entropy increases as the number of qubits increases and approaches unity asymptotically.

3.3 Chapter summary

In this chapter we introduced and explored the idea of universality of X-states. We reviewed a series of results that have recently led to a concrete proof that among two-qubits the X-states are universal. The immediate conjecture that follows is whether this result can be extended to more than two-qubits. Here we encounter an immediate obstacle that is for general N-qubit states there currently exists no conclusive procedure to determine whether a state is entangled and if so, how much. Thus even the numerical explorations that was a starting point for the case of two qubits is not feasible at the moment.

The all-party concurrence formula for X-states, however, provide an avenue to further explorations. One can ask similar questions that was raised about maximally entangled mixed states and only answer them for X-states. Questions such as what are the maximally entangled mixed states for a given purity or spectrum. What unitary transformation does maximize the entanglement of a given X-state? Such questions are at least amenable to numerical explorations. One can extend previous results by hypothesizing and then numerically check for the validity of such hypotheses and finally undertake an effort to prove them rigorously. This chapter was an example of such progress.

We found the class of N-qubit X-states that has the maximum all-party entanglement for a given value of mixedness. We showed that these states, named X-MEMS here, are a natural extension of their two qubit counterparts. We also found the critical entropy above which no X-state possesses genuinely multipartite entanglement. If the conjecture of universality of holds for more than two qubits, then the X-MEMS that are found here are indeed maximally entangled mixed states for all N-qubit states. It also interesting and open question to find the MEMS for different measures of all-party entanglement.

In the next chapter we shift our attention to a separate issue. We will try to deal with the problem of noise in experimental setups. Since noise is unavoidable producing highly idealized states such we discussed above can be very difficult if not impossible. We will try to develop bounds that give an estimate of the entanglement when it is only nearly is the ideal state of interest.

Chapter 4

Entanglement of experimental X-states

In the two previous chapters we derived a formula for the all-party concurrence of X-states and utilized this result to explore the relation between entanglement and different quantities in the Hilbert space. Here we explore a different aspect of the problem. Let us step back and see the problem in a larger context. Quantifying the all-party entanglement is a challenge. Previous studies have produced witnesses and/or lower bounds of the all-party entanglement [25, 26, 27, 28, 29, 30, 31, 32, 29, 28]. Many of these results are not well suited for use in experimental settings because they apply only for idealized noise-free states [30, 31, 32, 29], require numerical methods only feasible for few-partite systems [28], or require knowledge of the density operator of the state under test [25, 26]. The latter requirement is a problem for multi-party systems because, in general, the number of measurements to determine the density operator scales exponentially with the number of parties [33]. Apart from these methods, the measured value of witness operators can be used to find a lower bound for the entanglement realized in an experiment [34, 35, 36, 37]. Nonetheless, the efficacy of this approach for producing non-trivial lower bounds is not guaranteed, and complementary techniques are desired. In summary, quantifying all-party entanglement remains a challenge. Here we develop an approach that aims addressing this problem at least in a restricted way.

We will introduce a measure of all-party entanglement and find upper and lower bounds for the value of this measure. Our bounds do not require a full state tomography of the state and are experimentally relevant even for very large Hilbert spaces.

We will show that our bounds are specially useful for states that are nearly GHZ-diagonal. We finish the chapter with an example of the utility of our bounds in a real experimental settings.

4.1 The challenge of nearly ideal states

Let us discuss our challenge from a slightly different perspective. Assume that we are interested in producing a specific X-state in the laboratory. We design our experiment, put the setup together and start our characterization. Yet as much as we try to produce that ideal state there is always some noise left in the coherence elements. and thus what is created is not an ideal X-state. So we cannot take advantage of the algebraic formula that we derived to quantify its entanglement.

Yet entanglement is a continuous property of the state. It is highly non-linear function of the state but it is reasonable to assume that it is continuous. So we expect that for states that are nearly ideal with a very small noise, the measure of entanglement is nearly the same thing. It is this notion that we are going to characterize rigorously in this following sections.

One needs to first define what we mean by nearly ideal. How do we decide that two states are very close to each other? There are different distance measures for two states. Three famous candidates are fidelity, relative entropy, and trace distance, and a review of their properties can be found here [5]. We choose to work with the trace distance since it has all the nice properties of a measure. The trace distance of two matrices is defined by

$$D(\sigma,\rho)=\frac{1}{2}Tr|\rho-\sigma|=\frac{1}{2}Tr|\sigma-\rho|=D(\rho,\sigma) \tag{4.1.1}$$

where we define $|A|=\sqrt{AA^{\dagger}}$, is the sum of all singular values of A. Let us summarize the properties of this distance measure that we are going to use in the next section. Trace distance is invariant under unitary transformation:

$$D(U\rho U^{\dagger},U\sigma U^{\dagger})=D(\rho,\sigma). \tag{4.1.2}$$

The trace distance satisfies the triangle inequality

$$D\left(\rho,\sigma\right)\leq D(\rho,\tau)+D(\tau,\sigma) \tag{4.1.3}$$

There are two more properties of the trace distance that we will use in the next section to define a measure of all-party entanglement. First the trace distance is a convex quantity, thus for two probability distribution $\{p_i\}$ and $\{q_i\}$ and two sets of matrices ρ_i, and σ_i we will have

$$D\left(\sum_i p_i\rho_i, \sum_i q_i\sigma_i\right) \leq \frac{1}{2}\sum_i |p_i - q_i| + \sum_i D(\rho_i, \sigma_i) \tag{4.1.4}$$

The last property if the contractivity which is the following: Let $\mathcal{E}$ be a trace-preserving quantum operation, and ρ and σ are two density operators. Then

$$D(\mathcal{E}(\rho), \mathcal{E}(\sigma)) \leq D(\rho, \sigma). \tag{4.1.5}$$

Apart from the above properties we will use the fact that trace distance can be calculated simply in instances that are of interest to us. Before we close this section let us sketch out what we are going to do in the next section. We seek to attack the problem of nearly ideal state but first we needed to define what closeness of two states really mean. Now that we have that tool we also need to contemplate what measure of entanglement we are going to use? We have concurrence but it is defined through the idea of purity and the connection between purity and trace distance is not really clear. So what should we do? An answer to this challenge is presented in the next section.

4.2 Trace distance measure

One approach is to quantify the entanglement by a measure that is directly related to the trace distance. We are going to quantify the entanglement of a state by its distance from the set of non-entangled states [45]. For the all-party entangled the set of biseparable states is a convex set and one can quantify the all-party entanglement of any state to be the trace distance of that state with its closest biseparable state. In this section we first prove that trace distance provides a proper measure of entanglement and then provide an upper and a lower bound of this measure of entanglement that are based in the value of entanglement for close states. Let us introduce our measure of all-party entanglement to be,

$$\mathcal{E}(\rho) = \min_{\tau \in \mathcal{BS}} D(\rho, \tau), \tag{4.2.1}$$

where $\mathcal{BS}$ is the set of biseparable states. The trace distance is symmetric in its arguments and is zero if and only if its arguments are equal. The benefit of this approach, as we will show, lies in the fact that when we succeed in evaluating the measure for a given state, we can readily place tight bounds on the value of the measure for the states that are close to that state. Below we establish that $\mathcal{E}(\rho)$ is a monotone of the all-party entanglement.

To show that $\mathcal{E}(\rho)$ is an entanglement monotone we prove that $\mathcal{E}(\rho)$ is convex, non-increasing under local operations and classical communication (LOCC), and invariant under local unitary transformations. We first address the convexity of $\mathcal{E}(\rho)$, showing that $\mathcal{E}(\rho) \leq \lambda_1 \mathcal{E}(\rho_1) + \lambda_2 \mathcal{E}(\rho_2)$ if $\rho = \lambda_1 \rho_1 + \lambda_2 \rho_2$. If the two closest biseparable states to ρ_1 and ρ_2 are σ_1 and σ_2, respectively, then

$$\mathcal{E}(\rho_1) = D(\rho_1, \sigma_1), \quad \text{and} \quad \mathcal{E}(\rho_2) = D(\rho_2, \sigma_2). \tag{4.2.2}$$

The convexity of the trace distance allows us to conclude that

$$\begin{aligned} &\lambda_1 \mathcal{E}(\rho_1) + \lambda_2 \mathcal{E}(\rho_2) = \lambda_1 D(\rho_1, \sigma_1) + \lambda_2 D(\rho_2, \sigma_2) \geq \\ &D(\lambda_1 \rho_1 + \lambda_2 \rho_2, \lambda_1 \sigma_1 + \lambda_2 \sigma_2) = D(\rho, \sigma_{12}) \geq \mathcal{E}(\rho), \end{aligned} \tag{4.2.3}$$

where $\sigma_{12} = \lambda_1 \sigma_1 + \lambda_2 \sigma_2$ is biseparable, since the convex sum of any two biseparable states is itself a biseparable state.

To show that our measure is non-increasing under LOCC we use the contractive property of the trace distance [5]. The distance between two states cannot increase under trace-preserving quantum operations, i.e. for any two states, ρ and ρ'

$$D(\mathcal{M}(\rho), \mathcal{M}(\rho')) \leq D(\rho, \rho') \tag{4.2.4}$$

where $\mathcal{M}$ is a trace-preserving quantum operation. We note that any LOCC is a completely positive, trace-preserving map [71]. Now if the closest biseparable state to the state ρ is called σ then

$$\mathcal{E}(\rho) = D(\rho, \sigma) \geq D(\Gamma(\rho), \Gamma(\sigma)) \geq \mathcal{E}(\Gamma(\rho)) \tag{4.2.5}$$

where Γ is an LOCC. Note that in the last inequality, since σ is biseparable, any LOCC

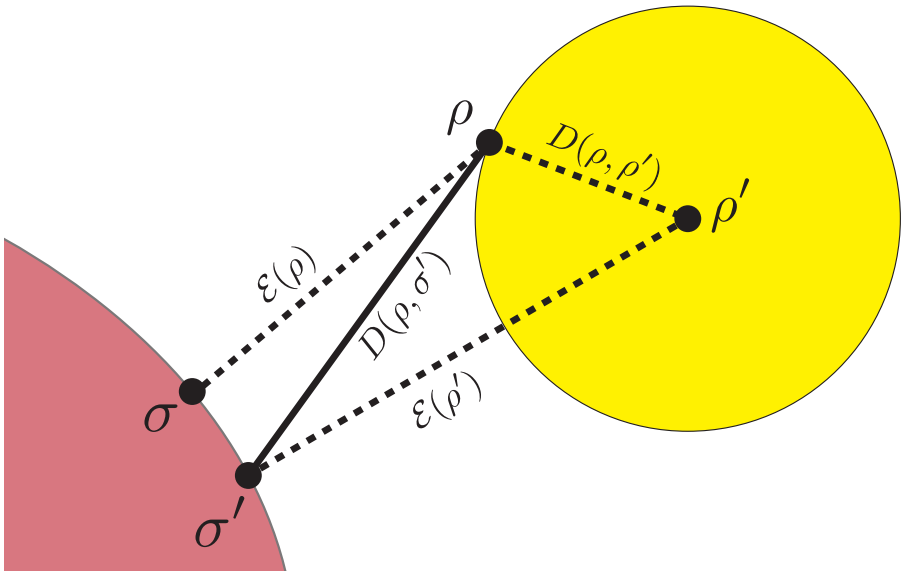

Figure 4.1: A graphic visualization of the bounds of entanglement. The red region represents the set of biseparable states. The yellow circle represents the set of states that are closer to ρ' than $D(\rho, \rho')$.

operation on it leads to another biseparable state.

Finally, we show that $\mathcal{E}(\rho)$ is invariant under local unitary transformations. Since the trace distance is invariant under unitary transformations [5], then

$$\mathcal{E}(\rho) = \min_{\tau \in \mathcal{BS}} D(U\rho U^\dagger, U\tau U^\dagger). \tag{4.2.6}$$

If U is a local unitary transformation then $\tau' = U\tau U^\dagger$ represents a one-to-one mapping between biseparable states, and we can write

$$\mathcal{E}(\rho) = \min_{\tau' \in \mathcal{BS}} D(U\rho U^\dagger, \tau') = \mathcal{E}(U\rho U^\dagger). \tag{4.2.7}$$

Thus, $\mathcal{E}$ is invariant under local unitary transformations. This completes our proof that $\mathcal{E}$ is an entanglement monotone.

4.2.1 Bounds on entanglement

Next we show that if the value of the entanglement measure is known for some state, one can use that value to bound the entanglement of other states. Later we will find the value of $\mathcal{E}(\rho)$ for all GHZ-diagonal states.

Let us assume we have a state ρ and another state ρ' for which we know the value

of $\mathcal{E}(\rho')$. Then there exist states σ and σ', the closest biseparable states to ρ and ρ', for which $\mathcal{E}(\rho) = D(\rho, \sigma)$ and $\mathcal{E}(\rho') = D(\rho', \sigma')$. Consequently we can conclude that

$$\mathcal{E}(\rho) = D(\rho, \sigma) \leq D(\rho, \sigma') \leq D(\rho, \rho') + D(\rho', \sigma') = D(\rho, \rho') + \mathcal{E}(\rho').$$

The last inequality is the result of the triangle inequality for our distance norm. The graphic picture in Fig. 4.1 can be helpful although our argument is purely algebraic. We can also find a lower bound for $\mathcal{E}(\rho)$ by employing the reverse triangle inequality;

$$\mathcal{E}(\rho) = D(\rho, \sigma) \geq D(\rho', \sigma) - D(\rho, \rho') \geq D(\rho', \sigma') - D(\rho, \rho') = \mathcal{E}(\rho') - D(\rho, \rho').$$

Consequently knowledge of $\mathcal{E}(\rho')$ allows us to bound the entanglement of ρ,

$$|\mathcal{E}(\rho) - \mathcal{E}(\rho')| \leq D(\rho, \rho'). \tag{4.2.8}$$

In fact, the upper bound in (4.2.8) can be tightened by noting that if σ' is known then

$$\mathcal{E}(\rho) \leq D(\rho, \sigma') \leq \mathcal{E}(\rho') + D(\rho, \rho') \tag{4.2.9}$$

as shown graphically by the solid line in Fig. 4.1. Finally, using the relationship between distance and fidelity [5],

$$D(\rho', \rho) \leq \sqrt{1 - F(\rho', \rho)^2}, \tag{4.2.10}$$

together with Eq. (4.2.8) and Eq. (4.2.9), we show that for any two states ρ, ρ':

$$\mathcal{E}(\rho') - \sqrt{1 - F(\rho', \rho)^2} \leq \mathcal{E}(\rho) \leq \sqrt{1 - F(\sigma', \rho)^2}, \tag{4.2.11}$$

where $\mathcal{E}(\rho)$ is the value of our entanglement measure for ρ, and $F(\rho', \rho)$ is the fidelity between ρ and ρ', and σ' is the closest biseparable state to ρ'. When ρ' is a GHZ state, the bounds in the above equation may be determined using only four measurements. The above bounds will be useful provided we can find another state close enough to ρ such that the bounds in Eq. (4.2.8) are non-trivial.

In deriving the above bounds we have not made any assumptions about the two states ρ and ρ'. Specifically, the value of the above bounds, and whether or not they are non-trivial, depends only on the distances (or fidelities) between states ρ and ρ'. For example if $D(\rho, \rho') < \mathcal{E}(\rho')$, the lower bound of entanglement becomes a non-trivial

positive value. A similar argument can be made for the upper bound. Next we will find the value of our measure for GHZ-diagonal states explicitly. This allows us to find bounds on the all-party entanglement of any state using its distance to a GHZ-diagonal state. But this does not mean that the bounds that we derived previously are only useful for states near to GHZ-diagonal states.

4.3 Entanglement of GHZ-diagonal states

We will now derive the value of $\mathcal{E}(\rho')$ for the so-called GHZ-diagonal states which are mixtures of GHZ states by finding the closest biseparable state, σ' to such states. We start with a definition and a lemma for N-qubit X-states [52], the class of N-qubit density matrices whose non-zero elements, in some orthonormal product basis, are diagonal and/or anti-diagonal. These matrices only have N-party coherences and tracing over any set of parties leads to a diagonal density matrix [63, 72].

Lemma: The closest biseparable state to an X-state is itself an X-state.

Proof: If we take a density matrix Y and map it to an X-state: $X = \chi(Y)$, by setting every element to zero except for the diagonal and anti-diagonal elements, it is shown in the Appendix that χ is an LOCC mapping. Let us assume the closest biseparable state to X, called X_{bs}, is not itself an X-state. The contractive property of the trace distance implies that

$$D(X, X_{bs}) \geq D(\chi(X), \chi(X_{bs})) = D(X, \chi(X_{bs})). \tag{4.3.1}$$

Also note that since X_{bs} is biseparable, so is $\chi(X_{bs})$. Thus if X_{bs} is not itself an X-state we can find a biseparable X-state that is closer to X than X_{bs}. This is in contradiction to the assumption that X_{bs} is the closest biseparable state to X. Thus we can conclude that the closest biseparable state to an X-state is itself an X-state.

Now we determine the closest biseparable state to the following X-state,

$$\hat{X}_N = \begin{pmatrix} a_1 & & & & & & z_1 \\ & b_2 & & & & z_2 & \\ & & \ddots & & \iddots & & \\ & & & b_n & z_n & & \\ & & & z_n^* & b_n & & \\ & & \iddots & & \ddots & & \\ & z_2^* & & & & b_2 & \\ z_1^* & & & & & & b_1 \end{pmatrix}, \tag{4.3.2}$$

where $n = 2^{N-1}$, and we require $|z_i| \leq b_i$, $|z_1| < \sqrt{a_1 b_1}$ and $a_1 + b_1 + 2\sum_i b_i = 1$ to ensure that $\hat{X}_N$ is positive and normalized. We further assume that $|z_1| \geq |z_i|$. The all-party concurrence of an N-qubit X-matrix is given by [32]

$$C(\hat{X}_N) = 2\max\{0, |z_1| - w_1\}, \tag{4.3.3}$$

where, for the X-states of the form in Eq. (4.3.2) $w_1 = \sum_{j\neq 1}^{n} b_j$. Notice that in the above X-state if $a_1 = b_1$, $\hat{X}_N$ becomes a GHZ-diagonal state. Below, we will show that the closest biseparable state to $\hat{X}_N$ has identical elements to X, except for z_1, which is replaced with $w_1 z_1/|z_1|$. Consequently the value of the all-party entanglement for X-states of the above form is given by

$$\mathcal{E}(\hat{X}_N) = \max\{0, |z_1| - w_1\}. \tag{4.3.4}$$

In the following we further assume $z_1 \in \mathbb{R}$ and $z_1 > 0$ since we can always change the phase of the basis to achieve this, and the distance is invariant under local unitary transformations. Furthermore we assume $z_1 = w_1 + \epsilon > w_1$, otherwise $\hat{X}_N$ is a biseparable matrix.

Let us parameterize the closest biseparable state to $\hat{X}_N$ to be $\hat{\Sigma} = \hat{X}_N + \hat{\Delta}$;

$$\hat{\Delta} = \begin{pmatrix} \delta_1^+ & & & & & & \nu_1 - \epsilon \\ & \delta_2^+ & & & & \nu_2 & \\ & & \ddots & & \iddots & & \\ & & & \delta_n^+ & \nu_n & & \\ & & & \nu_n^* & \delta_n^- & & \\ & & \iddots & & \ddots & & \\ & \nu_2^* & & & & \delta_2^- & \\ \nu_1^* - \epsilon & & & & & & \delta_1^- \end{pmatrix}, \tag{4.3.5}$$

The X form of the difference matrix implies that $D(\hat{X}, \hat{\Sigma}) = ||D_1|| + \sum_{i>1}^{n} ||D_i||$, where $||A|| = \frac{1}{2}\mathrm{Tr}|A|$ and

$$D_1 = \begin{pmatrix} \delta_1^+ & \nu_1 - \epsilon \\ \nu_1^* - \epsilon & \delta_1^- \end{pmatrix}, \quad D_i = \begin{pmatrix} \delta_i^+ & \nu_i \\ \nu_i^* & \delta_i^- \end{pmatrix}. \tag{4.3.6}$$

First we turn to the $||D_1||$ contribution. Taking advantage of the triangle inequality for the eigenvalues of D_1 leads to

$$||D_1|| \geq \frac{1}{2}\sqrt{(\delta_1^+ - \delta_1^-)^2 + 4|\epsilon - \nu_1|^2} \geq |\epsilon - Re(\nu_1)|.$$

Note that the above inequality implies that $Re(\nu_1) > 0$ since we assumed $D(\hat{X}_N, \hat{\Sigma}) < \epsilon$. Similarly using the triangle inequality for the eigenvalues of D_i, we can show that $||D_i|| \geq \frac{1}{2}|\delta_i^+ + \delta_i^-|$. Now we define $\delta_i = \frac{1}{2}(\delta_i^+ + \delta_i^-)$. We conclude

$$\sum_{i>1}(b_i + \delta_i) \geq \sum_{i>1}\sqrt{(b_i + \delta_i^+)(b_i + \delta_i^-)} \geq |w_1 + \nu_1| \geq w_1 + Re(\nu_1).$$

The second to last inequality arises from applying the condition of biseparability for the element $\hat{\Sigma}_{1,2n}$. Subtracting w_1 from both sides of the above equation leads to

$$\sum_{i>1}||D_i|| \geq \sum_{i>1}\delta_i \geq Re(\nu_1). \tag{4.3.7}$$

Thus we conclude that $D(\hat{X}, \hat{\Sigma}) = ||D_1|| + \sum_{i>1}^{n} ||D_i|| \geq \epsilon$. One can readily check that is inequality is saturated if $\hat{\Sigma}$'s elements are all identical to $\hat{X}_N$ except for z_1 that is

replaced with w_1. This completes our proof.

4.3.1 Experimentally accessible bounds

Now that we have proved Eq. (4.3.4), we need only show that if ρ' is a GHZ state then $F(\rho, \rho')$ and $F(\rho, \sigma')$ can be computed with four measurements regardless the number of qubits. That $F(\rho, \rho')$ depends only on the populations and coherences $\rho_{1,1}$, $\rho_{1,2n}$, and $\rho_{2n,2n}$ and therefore requires only four measurements has been shown previously [12, 8]. From our previous analysis we find that the nearest biseparable state to the GHZ state is $\sigma' = (|0\cdots0\rangle\langle 0\cdots0| + |1\cdots1\rangle\langle 1\cdots1|)/2$ for which it is easy to see that the fidelity, $F(\rho, \sigma')$, also only depends on the populations and coherences $\rho_{1,1}$, $\rho_{1,2n}$, and $\rho_{2n,2n}$.

In deriving the above experimentally more accessible bounds we took advantage of the fact that the fidelity between any state and a GHZ-state depends solely on three density matrix elements, i.e. $\rho_{1,1}$, $\rho_{1,2n}$, and $\rho_{2n,2n}$. An identical argument can be made even for GHZ-states that are not of equal weighting:

$$|\psi\rangle = \cos\theta|0,0,\ldots,0\rangle + \sin\theta|1,1,\ldots,1\rangle \tag{4.3.8}$$

Thus the lower bound of the entanglement can be improved using a simple optimization

$$\mathcal{E}(\rho) \geq \max_{\theta}\left(\frac{1}{2}|\sin 2\theta| - \sqrt{1 - F(\rho,|\psi\rangle)^2}\right) \tag{4.3.9}$$

where the fidelity reads

$$F(\rho,|\psi\rangle)^2 = \rho_{1,1}\cos^2\theta + \rho_{2n,2n}\sin^2\theta + \mathrm{Re}(\rho_{1,2n})\sin 2\theta \tag{4.3.10}$$

We demonstrate the utility of our approach by using the fidelities recently reported on the creation of GHZ-states among up to fourteen ions to establish lower bounds on the actual entanglement produced in the experiment [8]. The lower bounds on the generated all-party entanglement for states that are produced with up to six ions are given in Table 4.1. The fidelities of states with larger numbers of qubits are not big enough to establish non-trivial lower bounds. Regardless, these states are all-party entangled as reported by the authors.

Number of ions	2	3	4	5	6
Fidelity, %	98.6	97.0	95.7	94.4	89.2
$\mathcal{E}>$	0.33	0.25	0.2	0.17	0.044
$\mathcal{E}\%>$	66	50	40	34	8.8

Table 4.1: The lower bound $\mathcal{E}$ of the entanglement of the states reported in Ref. [8]. The third row is the percentage of the produced entanglement lower bound relative to the entanglement of a GHZ state.

4.4 Distance from the closest fully separable state

In this section we focus on the entanglement properties of a subclass of GHZ-diagonal states. The GHZ-diagonal states are themselves a subset of X-states. In our notation they are X-states for which $a_i = b_i$. Such matrices can be written as a convex sum of GHZ states, hence their name. The entanglement properties of GHZ-diagonal states has already been the subject of a few previous investigations [73, 25, 74, 65, 75].

For the purpose of the current section we impose an extra condition of $z_i = 0$ for $i > 1$. The states that we are interested in are X-matrices of the form given below.

$$\hat{\rho}_x = \begin{pmatrix} a_1 & & & & & & z_1 \\ & b_2 & & & & 0 & \\ & & \ddots & & \iddots & & \\ & & & b_d & 0 & & \\ & & & 0 & b_d & & \\ & & \iddots & & & \ddots & \\ & 0 & & & & b_2 & \\ z_1^* & & & & & & a_1 \end{pmatrix}. \tag{4.4.1}$$

The conditions for biseparability and full separability of all partitioning of such states are known [73]. For these states to be fully separable it is necessary and sufficient that

$$S = |z_1| - \min\{b_i\} \leq 0 \tag{4.4.2}$$

Below we show that the quantity S also has a simple geometrical interpretation and it can be used as a measure of weak inseparability. We submit that $S \geq 0$ is the distance from the closest fully separable state. The distance metric we are using here is the trace distance that we have used previously to find a measure of all-party entanglement

[76]. The trace distance of two matrices is given by

$$D(\rho,\tau)=\frac{1}{2}\mathrm{Tr}(|\rho-\tau|), \tag{4.4.3}$$

where $|A|=\sqrt{AA^{\dagger}}$. The measure of weak inseparability that we introduce here is

$$E(\rho)=\min_{\tau\in\mathcal{FS}}2D(\rho,\tau) \tag{4.4.4}$$

where $\mathcal{FS}$ denotes the set of fully separable states, which is a convex set. Identically to the proof we have given in previous sections we can show that $E(\rho)$ is convex, non-increasing under LOCC and invariant under local unitary transformations. From now on, unless otherwise said, we use separable in stead of fully separable. Now we prove the main result of this section that is to find the closest fully separable state to $\hat{\rho}_x$. It is shown in [73] that any density matrix can be depolarized to a state of the form $\hat{\rho}_x$ using an LOCC map. This and the contractive property of the trace distance guarantee that the closest separable state to $\hat{\rho}_x$ has the same form as $\hat{\rho}_x$. In the following we assume that $z_1=|z_1|$ without loss of generality since this can always be accomplished using a local unitary transformation without changing any other element of the matrix, and the distance is invariant under local unitary transformaitons. We assume $z_1=\min\{b_i\}+\epsilon>\min\{b_i\}=c$. We will prove that the closest separable state to $\hat{\rho}_x$ has identical elements except for z_1 replaced with with c, i.e. $E(\hat{\rho}_x)=\epsilon$.

To prove let us assume the contrary. There exists a separable state $\hat{\Sigma}$ that is closer to $\hat{\rho}_x$ than ϵ. We parameterize this state as $\hat{\Sigma}=\hat{\rho}_x+\hat{\Delta}$:

$$\hat{\Delta}=\begin{pmatrix} \delta_1 & & & & & & \nu-\epsilon \\ & \delta_2 & & & & 0 & \\ & & \ddots & & \iddots & & \\ & & & \delta_d & 0 & & \\ & & & 0 & \delta_d & & \\ & & \iddots & & \ddots & & \\ & 0 & & & & \delta_2 & \\ \nu^*-\epsilon & & & & & & \delta_1 \end{pmatrix}. \tag{4.4.5}$$

The X form of the difference matrix implies that $D(\hat{\rho}_x,\Sigma)=\frac{|D_1|}{2}+\Sigma_{i>0}|\delta_i|$.

$$D_1 = \begin{pmatrix} \delta_1 & \nu_1 - \epsilon \\ \nu_1^* - \epsilon & \delta_1 \end{pmatrix} \tag{4.4.6}$$

The contribution from D_1 leads to

$$\frac{|D_1|}{2} \geq |\epsilon - \nu| \geq |\epsilon - \Re(\nu)|. \tag{4.4.7}$$

The above inequality implies that $\Re(\nu) > 0$ since we assumes that $D(\hat{\rho}_x, \Sigma) < \epsilon$. Since Σ is a separable state we should have that for all i's

$$b_i + \delta_i \geq |c + \nu| \geq c + \Re(\nu). \tag{4.4.8}$$

Let $i = j$ be the index for which $b_j = c$, then $\delta_i \geq \Re(\nu)$. Thus we have $D(\hat{\rho}_x, \Sigma) \geq |D_1| + \delta_i \geq \epsilon$. This implies that there is no separable state closest to $\hat{\rho}_x$ than $z_1 - c$. The state with $\delta_i = 0$ and $\nu = 0$ saturates this inequality and thus $E(\rho) = \min\{|z_1| - c, 0\}$. In the thesis we choose the normalization $S = 2E(\hat{\rho}_x)$ so that the distance matches the value of the all-party concurrence for $\hat{\rho}_x$.

4.5 Chapter summary

More than a century after the seminal work of Schmidt [2], and inspite of important contributions from many, including Werner [77] and Wootters [20], to the theory of entanglement, the question of how to determine and quantify the entanglement of a given state remains open. Of particular importance is determining the all-party entanglement among many qubits in an experimental setting. This is a difficult problem because most presently available techniques are not well suited for experimentally produced systems in which noise is always present. Additionally, the exponential scaling of measurements required to determine the state of N-qubits make state-based approaches very inefficient. Finally, witness-based techniques for quantifying the entanglement do not currently provide upper bounds and may not result in non-trivial lower bounds.

In this chapter, we have introduced a technique to solve this problem by using a distance measure to derive bounds on the all-party entanglement for an arbitrary number N of qubits. We derived an algebraic formula for the all-party entanglement of

GHZ-diagonal states and then used this formula to derive easily calculable upper and lower bounds to the all-party entanglement of any experimentally produced state based on the results of just four measurements. This is a particularly promising technique for establishing the bounds of the produced entanglement when N is large.

As mentioned in the beginning, we used our lower bound to quantify the non-zero all-party entanglement that was produced in a recent experiment [8]. We used the fidelities reported on the creation of GHZ-states of up to fourteen ions and established lower bounds on the actual all-party entanglement for states with up to six ions. The fidelities of states with larger numbers of qubits are not big enough to establish non-trivial lower bounds. Regardless, these states are all-party entangled as reported by the authors. While upper bounds appropriate to the experiment in [8] could also be computed from two of the populations and one of the coherences using our approach, the required populations were not reported.

So far in this thesis we focused on the question regarding how to determine a state is separable or entangled, how to quantify this entanglement and how to sharpen our methods for experimental techniques or use or insight to explore the connection between different quantities in large Hilbert spaces. In the final chapter we change our focus to the the dynamics of entanglement. How it is being lost and is there a way to exert some control over all-party entanglement among many parties.

Chapter 5

Multipartite entanglement in open systems

So far in this work we focused on questions regarding how to determine whether a given state is entangled, and if so how to properly quantify such an entanglement. We developed an algebraic formula for the all-party concurrence of N-qubit X-states and explored the relation between linear entropy and all-party concurrence. In the last chapter we presented a discussion on a distance measure of entanglement and how to utilize it to develop bounds on all-party entanglement that are directly accessible in an experimental settings without the need to characterize the state completely.

In this chapter we utilize the machinery that we have developed in the previous chapters to study the dynamics of multipartite entanglement in an explicitly quantitative approach. In the first part of the chapter we study the dynamics of multipartite entanglement in open systems that are experiencing local decoherence. We also present a short discussion on the robustness of such entanglement against white noise.

In the second half of this chapter we focus on an approach to defeat the suppression of entanglement in a controlled setting. Our approach uses the phenomenon of collapse and revivals to coherently suppress and revive the multipartite entanglement. Multipartite entanglement can signal inseparability for different partitionings of the system. Here we examine two extreme kinds of entanglement: (i) all-party entanglement, also known as genuinely multipartite entanglement, which signals inseparability along all possible partitionings, and (ii) weak inseparability, defined as the lack of full separability. Full separability signals that the state is not entangled along any partitioning. We develop an approximation that allows us to obtain analytical expressions

for both of these quantities.

The qubits are initially assumed to be in a Greenberger-Horne-Zeilinger (GHZ) state [9] and we explain below an approximation that reduces their density matrix to an X-state for all times. X-states are N-qubit density matrices whose non-zero elements are restricted to diagonal or anti-diagonal in an orthonormal product basis. They include important states such as GHZ and GHZ-diagonal states. Our approximation enables us to use the algebraic formula developed previously in chapter three to quantify the all-party entanglement. We also utilize the distance from the set of fully-separable states as our measure of weak inseparability. We obtain an analytical formula for this quantity during dynamics. We observe that beyond three qubits the initial loss of all-party entanglement after collapse is permanent. We then examine weak inseparability, and demonstrate that, contrary to all-party entanglement, weak inseparability experiences revivals even for very large values of N, although the strength of such revivals decreases with N. Our result suggests a clear picture of the path that the N-qubit state traverses during the dynamics.

5.1 Local decoherence channels and all-party entanglement

In this section we investigate two examples of all-party entanglement dynamics in open systems. Our first example is the all-party entanglement in a system that experience decoherence through N local amplitude damping channel. Earlier studies to tame this problem have only been successful qualitatively [78]. Here we present a completely quantitative approach and determine how entanglement changes through the dynamics.

One feature that typically companies the dynamics of entanglement in open systems is the non-exponential disappearance of entanglement in finite time that was first identified by Yu and Eberly [52, 51], the entanglement sudden death. Here we study which states experience entanglement sudden death.

5.1.1 Robustness of N-partite entanglement

Restricted forms of X-matrices of more than two qubits have been used in some recent studies of the dynamics of multipartite entanglement. The entanglement measures utilized in these studies yield qualitative information about the multipartite entanglement

[79, 80, 81, 82]. Direct study of the dynamics of genuinely multipartite entanglement has been an elusive problem mainly due to the lack of an analytical measure of genuinely multipartite entanglement that is simple to calculate. Our GM concurrence formula provides an opening to quantitatively examine the conjectures of such studies and many other scenarios whenever the initial density matrix is an X-matrix and the X nature of the density matrix is robust in the dynamics.

In the following we use our formula to directly study the dynamics of the multiqubit entanglement shared by N qubits when each qubit is subjected to a local amplitude damping channel. This can represent, for example, the spontaneous decay of N two-level atoms, each in a separate zero-temperature Markovian reservoir. For a two-level atom in zero-temperature Markovian reservoir, the evolution of ground and excited states, $|g,0\rangle$ and $|e,0\rangle$, is given by

$$\begin{aligned} U(t)|e,0\rangle &= A_t|e,0\rangle + B_t|g,\mathbf{1}\rangle, \\ U(t)|g,0\rangle &= |g,0\rangle, \end{aligned} \tag{5.1.1}$$

where $U(t)$ is the local propagator, $A_t = \sqrt{1-P_t}$, and $B_t = \sqrt{P_t}$. Although P_t has a time dependence $P_t = 1 - e^{-\gamma t}$ where γ is the damping rate, we can also think of P_t as the probability of the decay and write everything as a function of P instead of an explicit dependence on time. Thus, in the following we drop the explicit time dependence of P. The state $|\mathbf{1}\rangle$ denotes an excited state of a local reservoir.

We study the dynamics of the multiqubit entanglement that is shared initially by N-partite GHZ states:

$$|\Phi_N^{(k)}, \alpha\rangle = \cos\alpha|e^{\otimes N-k}g^{\otimes k}\rangle + \sin\alpha|g^{\otimes N-k}e^{\otimes k}\rangle$$

This is a GHZ state where either $(N-k)$'s of the qubits are initially excited and the rest are in their ground state or k qubits are initially excited and the rest are in their ground states. We first study the $k=0$ case. We present a detailed analysis only for the three qubit case but the generalization to N qubits is straightforward. By tracing

out the reservoirs we find the density matrix of the three atoms,

$$\hat{\rho}_{\Phi_3^{(0)}}(t) = \begin{pmatrix} a_1 & & & & & & & z_1 \\ & a_2 & & & & & & \\ & & a_2 & & & & & \\ & & & b_2 & & & & \\ & & & & a_2 & & & \\ & & & & & b_2 & & \\ & & & & & & b_2 & \\ z_1 & & & & & & & b_1 \end{pmatrix}, \tag{5.1.2}$$

where

$$\begin{aligned} a_1 &= \cos^2\alpha |A_t|^6, & b_1 &= \sin^2\alpha + \cos^2\alpha |B_t|^6, \\ a_2 &= \cos^2\alpha |A_t^2 B_t|^2, & b_2 &= \cos^2\alpha |A_t B_t^2|^2, \\ z_1 &= \sin\alpha\cos\alpha A_t^3. \end{aligned}$$

For an initial $|\Phi_N^{(0)}, \alpha\rangle$ state the concurrence reads

$$\begin{aligned} C_N^{(0)} &= \max\{0, Q_N^{(0)}\}, \\ Q_N^{(0)} &= 2(\cos^2\alpha)\ (1-P)^{\frac{N}{2}} \left(|\tan\alpha| - (2^{N-1}-1)P^{\frac{N}{2}} \right). \end{aligned} \tag{5.1.3}$$

In Fig. 5.1, we plot $Q_N^{(0)}$ versus P for $N = \{2, 10, 100\}$ qubits. It confirms that the bulk of the initial entanglement dies out faster (at smaller P's) as the number of qubits increases. In the $Q_N^{(0)}$ formula, the non-negative factor, $2(\cos^2\alpha)\ (1-P)^{\frac{N}{2}}$, determines the decay of entanglement for $N \gg 2$, and one can show that for the amplitude damping channel the half-life of the entanglement depends on N as

$$P_{\text{half-life}} \approx \frac{2\log 2}{N}, \tag{5.1.4}$$

which is the same as the half-life of the coherence elements in the density matrix. We observe from Fig. 5.1 that the half-life of the entanglement decreases as the number of the qubits increases. One might expect a similar dependence on N for the time at which the entanglement disappears completely. However, this is not always the case. In order to show this we solve the equation $Q_N^{(0)} = 0$ for the critical value of P, beyond

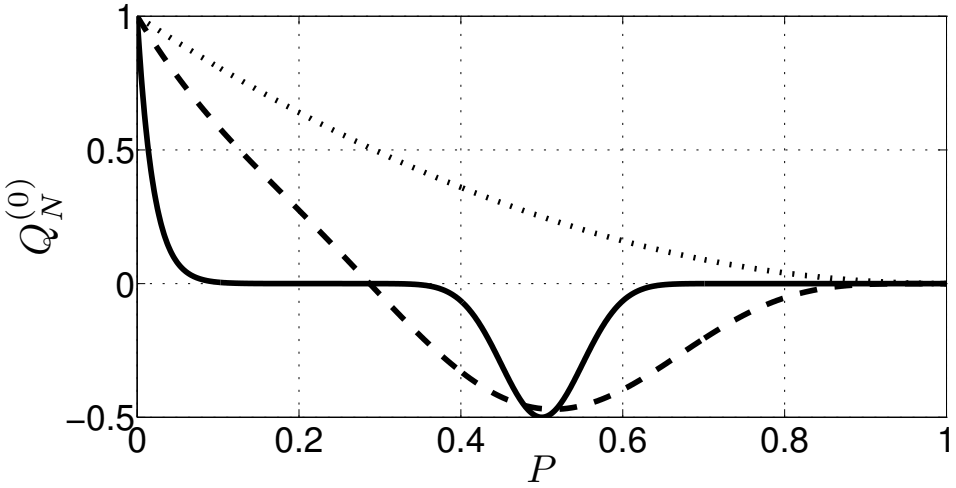

Figure 5.1: The $Q_N^{(0)}$ vs P for different numbers of qubits for the initial state $|\Phi_N^{(0)}, \frac{\pi}{4}\rangle$. $N = 2$ is the dotted line, $N = 10$ is the dashed line and $N = 100$ is the solid line.

which the concurrence is zero:

$$P \geq \left(\frac{|\tan\alpha|}{2^{N-1}-1}\right)^{\frac{2}{N}} = P_c. \tag{5.1.5}$$

If $P_c < 1$, then the entanglement has a finite life [51]. Otherwise the entanglement dies out asymptotically. In Fig. 5.2, we plot P_c versus the number of the qubits for different initial states. We observe that the critical value, P_c, can increase, decrease or even decrease and then increase as a function of N. The parameter that determines this peculiar dependence of P_c on N is $\tan\alpha$, which one can think of as a distance of the initial state to the final state. In the macroscopic limit, $N \to \infty$, even this dependence on $\tan\alpha$ is suppressed. Thus although the half-life of macroscopic entanglement is very small, a non-zero entanglement lasts for a constant interval of time before vanishing completely.

Similar unusual behaviors were observed by Aolita *et al.* [78] for the entanglement of different bipartitions of N qubits. They had derived similar N-dependence for the half-life and also provided examples of initial states giving P_c increasing with N. It should be pointed out that since the entanglement of different bipartitions is not a sufficient condition for N-partite entanglement similar behavior was not a foregone conclusion.

For the $k > 0$ case one can show that the initial entanglement only decays asymp-

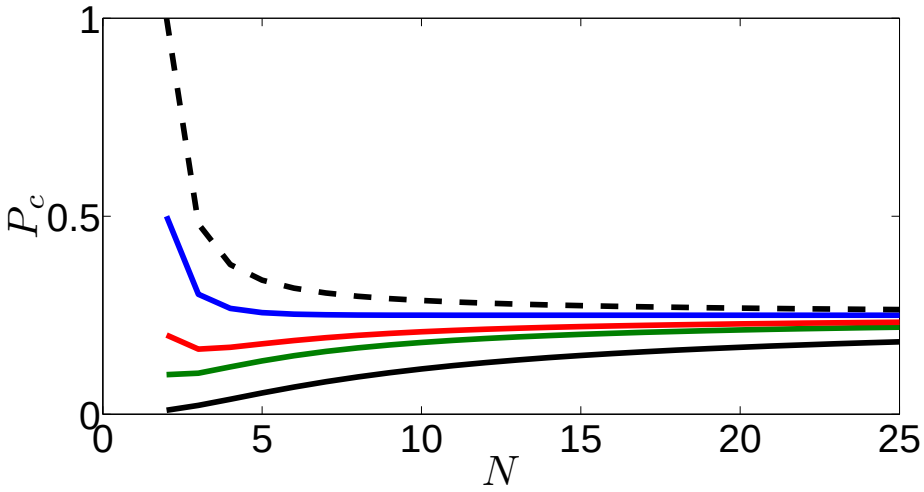

Figure 5.2: P_c vs number of qubits for different initial states $|\Phi_N^{(0)}, \alpha\rangle$. From bottom up $\tan\alpha = 0.01, 0.1, 0.2, 0.5$, and 1 respectively.

totically. Below we present the argument for $N = 3$ and $k = 1$ but the extension to higher N is straightforward. The asymptotic decay of entanglement is due to the fact that $\langle e,e,e|\rho_{\Phi_3^{(1)}}|e,e,e\rangle$, $\langle e,g,e|\rho_{\Phi_3^{(1)}}|e,g,e\rangle$, and $\langle g,e,e|\rho_{\Phi_3^{(1)}}|g,e,e\rangle$ remain zero for all times. To show this, we note that our initial state is a superposition of two possibilities. Either two of the atoms, $\{1,2\}$, are excited and the other atom, $\{3\}$, is in vacuum state, or that single atom is excited and the atoms $\{1,2\}$ are in their ground states. Since all reservoirs are initially in their ground states, if an atom is in its ground state initially it will always remain there. The three diagonal terms that we referred to require the atom $\{3\}$ and at least one of the other two atoms to be excited simultaneously. Since this is forbidden, all of these matrix elements remain zero. Thus the negative contribution to the concurrence formula remain zero. This argument can be generalized for $N \geq 4$ to all of the GHZ states except for $|\Phi_N^{(0)}, \alpha\rangle$, because in the $|\Phi_N^{(0)}, \alpha\rangle$ state all of the atoms can be initially excited. The concurrence of all $|\Phi_N^{(k)}, \alpha\rangle$ initial states with $k > 0$ is given by

$$C_N^{(k)} = |\sin 2\alpha|(1-P)^{\frac{N}{2}}.$$

Thus for $k > 0$, concurrence only dies when $P = 1$.

The entanglement that is stored initially between the N qubits is transferred to the environments. Since the environments in this case also remain qubits we can also try

to study the entanglement between different environments. From the above equations for the state at all times one can trace out the atoms and find the density matrix of different environments. One can readily check the result is a density similar to that of the atoms with A_t's are exchanged with B_t's. This is equivalent to exchanging P and $1-P$ in the concurrence formula. For the initial state of $|\Phi_N^{(0)}, \alpha\rangle$, the concurrence between different environments is given by

$$\begin{aligned} C_{Ne}^{(0)} &= \max\{0, Q_{Ne}^{(0)}\}, \\ Q_{Ne}^{(0)} &= 2(\cos^2\alpha)\ P^{\frac{N}{2}} \left(|\tan\alpha| - (2^{N-1}-1)(1-P)^{\frac{N}{2}} \right). \end{aligned} \tag{5.1.6}$$

The plot for the all-party concurrence among the environments is identical to the plot of all-party concurrence among the atoms mirrored along the P access. We previously saw that as the number of parties increases the entanglement is lost faster in strength. Here we observe the opposite perspective that as N increases the transfer of the bulk of the entanglement to all-party entanglement among the environments happens later.

5.1.2 Robustness against white noise

We now study robustness of the entanglement agains white noise. Adding white noise (a maximally mixed state) to the density matrix does not change the X nature of the density matrix, so we look at a density matrix of the form

$$\hat{Y} = (1-p)\hat{X} + \frac{p}{2^N}\hat{I}, \tag{5.1.7}$$

where $\hat{I}$ is the identity matrix, p is the mixing parameter, and we again assume $\sqrt{a_1 b_1} \geq \sqrt{a_i b_i}$. The diagonal and cross diagonal elements change according to

$$\begin{aligned} a_i &\longrightarrow (1-p)a_i + \frac{p}{2^N}, \\ b_i &\longrightarrow (1-p)b_i + \frac{p}{2^N}, \\ z_i &\longrightarrow (1-p)z_i, \\ w_i &\longrightarrow (1-p)w_i + \sqrt{\frac{p(1-p)}{2^N}(1-a_i-b_i)} + (\frac{1}{2} - \frac{1}{2^N})p, \end{aligned} \tag{5.1.8}$$

The concurrence of $\hat{Y}$ reads

$$C(\hat{Y}) = 2\max\{0, (1-p)(|z_1| - w_1) - \sqrt{\frac{p(1-p)}{2^N}(1-a_1-b_1)} - (\frac{1}{2} - \frac{1}{2^N})p\}. \tag{5.1.9}$$

The third term on the right hand side is independent of the density matrix $\hat{X}$. The second term depends on the density matrix and vanishes for the GHZ states. Thus amongst X-matrices of N qubits, the GHZ states are the most robust. The entanglement of a maximally entangled GHZ states disappears when

$$p \geq \frac{2^{N-1}}{2^N - 1} = p_{bisep}. \tag{5.1.10}$$

In Fig. 5.3, we plot the concurrence of a maximally entangled GHZ state mixed with maximally mixed state versus p for two extremal value of $N = \{2, \infty\}$. It is interesting to note that the N-partite concurrence of the maximally entangled GHZ state dies out linearly with a rate between -2 and $-\frac{3}{2}$. Comparing this result with that of amplitude damping we can conclude that in handling N-partite entanglement, amplitude damping is a more important source of entanglement decay than exposure to white noise.

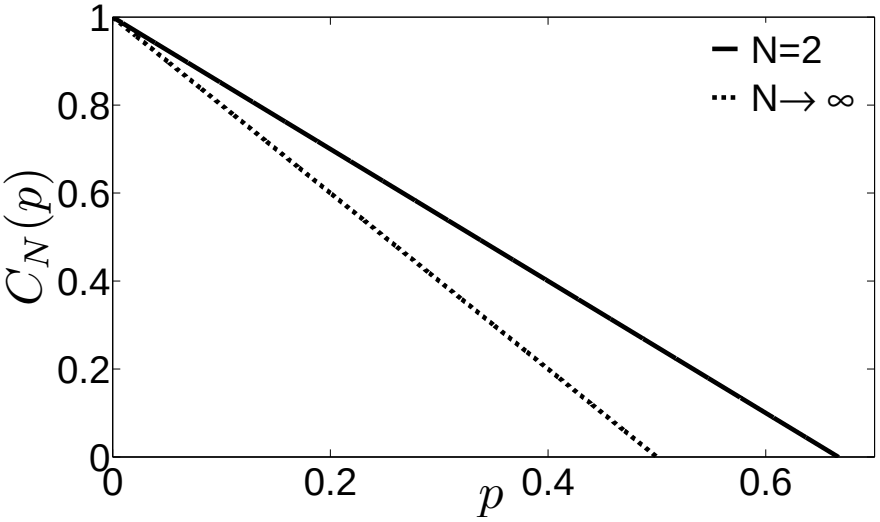

Figure 5.3: C_N versus p for two extremal value of $N = \{2, \infty\}$, $\tan\alpha = 1$ (a maximally entangled GHZ state).

5.2 Coherent control of multipartite entanglement

Three important aspects of any quantum technology are the creation, characterization and controlled preservation of entanglement in settings involving a large number of parties. Efforts to produce entanglement among many parties have led to the observation of multipartite entanglement among up to fourteen ions [8]. An emerging field of study, compressive quantum state tomography, could also be helpful in experimental characterization of such states even for large numbers of parties. In this approach the prior knowledge that the state produced in an experiment is close to some ideal state can be used to characterize the experimental state with a number of measurements that grows slower than quadratically for conventional quantum state tomography [83, 84]. There are also a few approaches to preserve the entanglement such as the quantum Zeno effect [85], entanglement distillation [39, 86, 87, 88] or weak measurements [89]. Unfortunately such schemes usually lack an element of control and/or their success is probabilistic.

In this section we will present a scheme for controlled entanglement preservation. The scheme can be applied to systems of arbitrary number of qubits, and its success is deterministic. We will show that our all-party concurrence formula allows us to examine our new scheme quantitatively.

We combine knowledge about N-party entanglement with control of revival dynamics to demonstrate quantitative control of multipartite entanglement. Elements of our procedure have only been exploited for two-qubits previously [90]. We present an example of multipartite entanglement that is initially shared by N remote qubits interacting with individual fields. Local control is managed by a coherent state of a resonant mode via collapse and revivals of the qubit coherences. By controlling the amplitude of the coherent states one controls the time of revivals and thus the recovery of the multi-qubit entanglement. We note that entanglement and revivals were previously discussed in studies focused on the entanglement of one qubit and its local field [91, 92]. Here, we mean the entanglement among the qubits and not inseparability from their local fields. A schematic representation of the scenario that we are interested in is presented in Fig. (5.4)

In the following, we first briefly revisit the theory of collapse and revivals in JC model [93]. We then shortly discuss the possibility of experimental realization of our scheme. Then we present our calculation of the all-party concurrence and its implications.

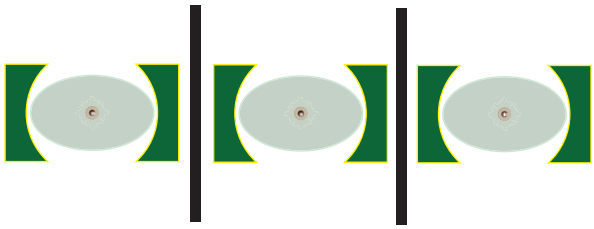

Figure 5.4: Schematic representation of three subsystems each composed of a two-level system inside a single mode cavity.

5.2.1 Collapse and revivals in the Jaynes-Cummings model

The system under our investigation is made of N remote (non-interacting) subsystems. All subsystems are assumed to be identical. Each subsystem is made of a two-level system (a qubit) that is interacting with a single mode of the electromagnetic field through a Jaynes-Cummings interactions [94].

$$H_i = \frac{\omega_0}{2}\sigma_{zi} + g(a_i^\dagger \sigma_i^- + a_i \sigma_i^+) + \omega a_i^\dagger a_i \tag{5.2.1}$$

The frequencies and the coupling constants are identical for all subsystems. The Jaynes-Cummings Hamiltonian is integrable and one can analytically follow the evolution of the above model. First we follow the dynamics of Jaynes-Cummings model for Fock states.

For start let us assume that each of the qubits is interacting with a Fock state of n excitations. Using the Jaynes-Cummings model the evolution of each subsystem is given by.

$$\begin{aligned} U_t|e,n\rangle &= |e,n\rangle_t = r_{n+1}|e,n\rangle + t_{n+1}|g,n+1\rangle \\ U_t|g,n\rangle &= |g,n\rangle_t = t_n|e,n-1\rangle + r_n|g,n\rangle \end{aligned} \tag{5.2.2}$$

where for $n > 0$, $r_n = e^{-in\omega t}\cos(g\sqrt{n}t)$ and $t_n = -ie^{-in\omega t}\sin(g\sqrt{n}t)$.

Now we turn to the more complex case of coherent states. For simplicity we assume that α is real and positive.

$$|\alpha\rangle = \sum_n e^{-\alpha^2/2}\frac{\alpha^n}{\sqrt{n!}}|n\rangle = \sum_n A_n|n\rangle.$$

We can write the coherently driven evolution of $|e\rangle$ and $|g\rangle$ states:

$$|e,\alpha\rangle_t = \sum_n A_n |e,n\rangle_t = |e\rangle \otimes |\phi_0\rangle + |g\rangle \otimes |\phi_1\rangle \tag{5.2.3}$$

where

$$|\phi_0\rangle = \sum_n A_n r_{n+1} |n\rangle, \qquad |\phi_1\rangle = \sum_n A_n t_{n+1} |n+1\rangle \tag{5.2.4}$$

and

$$|g,\alpha\rangle_t = \sum_n A_n |g,n\rangle_t = |e\rangle \otimes |\phi_2\rangle + |g\rangle \otimes |\phi_3\rangle \tag{5.2.5}$$

where

$$|\phi_2\rangle = \sum_n A_n t_n |n-1\rangle, \qquad |\phi_3\rangle = \sum_n A_n r_n |n\rangle. \tag{5.2.6}$$

All the dynamics we intend to investigate can be captured by the inner products of these four different $|\phi_i\rangle$'s. For $\alpha \geq 10$ excellent approximations are available to evaluate these inner products (Appendix A). The summary of the results is given below.

$$\begin{aligned}
&\langle\phi_i|\phi_i\rangle = \frac{1+p_1 x}{2}, && p_1 = \begin{cases} +1 & i=0,3 \\ -1 & i=1,2 \end{cases} \\
&\langle\phi_i|\phi_{i+1}\rangle = i\frac{e^{i\omega t}}{2}(I_2 + p_2 y), && p_2 = \begin{cases} +1 & i=2 \\ -1 & i=0 \end{cases} \\
&\langle\phi_i|\phi_{3-i}\rangle = \frac{e^{i\omega t}}{2}(I_1 + p_3 x), && p_3 = \begin{cases} +1 & i=2 \\ -1 & i=0 \end{cases} \\
&\langle\phi_0|\phi_2\rangle = -\langle\phi_1|\phi_3\rangle = -\frac{iy}{2}
\end{aligned}$$

where $x + iy = \sum_n A_n^2 \exp(2igt\sqrt{n})$, and

$$I_1 + iI_2 \simeq \exp(-\frac{g^2 t^2}{32\alpha^4}) e^{\frac{igt}{2\alpha}}. \tag{5.2.7}$$

A detailed derivation of the above results and evaluations of the four quantities are given in Appendix A. In Fig. 5.5 we present the time dependence of x, I_1, and I_2 for the coherent states with $\alpha = 10$. The plot for y is similar to the plot for x except

that the fast Rabi oscillations in the revivals are π out of phase. At the first revival the maximum of $|x|$ is $\frac{1}{2}$, and $I_1 \simeq -1$. At all revivals $I_2 \simeq 0$.

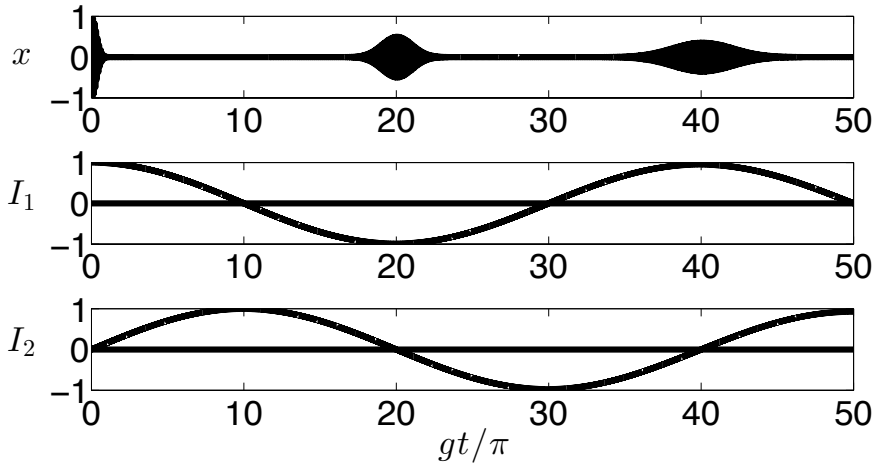

Figure 5.5: The time dependence of x, I_1, and I_2 for coherent states of $\alpha = 10$.

Revivals are especially prominent since their presence is a direct result of a discrete photon distribution [93]. To observe revivals one has to prepare a cavity with a small leakage constant such that until the first revival the chance of losing a photon is negligible. Since we are dealing with N cavities, to observe revivals in the entanglement dynamics we have to make sure that no photon leaks out from any of the cavities until the first revival time. This will lead to a leakage constant that is N times smaller than the leakage constant needed to observe a revival in a single cavity. For a coherent state of, on average, hundred photons the ratio of coupling constant to the decay rate of 10^3 is required to observe the revival in a single cavity, which is not outrageously higher than 3×10^2 that was achieved in a circuit QED setup recently [95]. Thus only an order of magnitude improvement in this ratio leads to suitable condition for revival of multipartite entanglement in a setup with $N \geq 3$. In the following, we assume this condition is satisfied and ignore the leakage of the cavities altogether.

5.2.2 Density matrix and X-approximation

Before computing the entanglement we need to find the density matrix. In deriving the density matrix we are going to use an approximation that leads to a GHZ-diagonal

state. Thus we can use the X-state formula to study the dynamics of the entanglement. In deriving the density matrix, we follow the same approximation that was developed in [90].

To decide which elements of the matrix can be safely discarded Yönaç and Eberly [90] replaced $|\alpha\rangle$ by $|\bar{n}\rangle$ where $\bar{n} = \alpha^2$. This replacement is at least weakly supported by the fact that for $\bar{n} \gg 1$ the photon distribution of a coherent state is relatively narrowly peaked around $\bar{n}$. One can instead assume a less extreme variant of this approximation where $|\alpha\rangle$ is replaced by a mixture of Fock states $|n\rangle$ that has the same photon distribution as $|\alpha\rangle$. Both of these approximations leads to one important consequence. If the qubits are initially in a GHZ-state, then we will have a density matrix whose non-zero elements are either diagonal or anti-diagonal. Furthermore, This density matrix will have only one non-zero anti-diagonal element. We then calculate the values of non-zero elements using their values from a coherent state. In fact the simplification goes even further and we will show that $a_i = b_i$. This will guarantee that, if the initial state is a GHZ states, the density matrix remains a GHZ-diagonal matrix. The above approximation is shown to be an excellent choice in capturing the collapse and revivals [96, 90]. This approximation also enables us to calculate a proper measure of inseparability as we have shown in Appendix B.

Before closing this subsection let us emphasize that the above approximation is equivalent to ignoring all non-diagonal elements except of one them in the outset. Thus all the estimates that we are deriving are guaranteed to be lower bounds to the actual value. The above justification implies that this lower bound is approximately the actual value of the concurrence [32, 75].

5.2.3 Entanglement revival dynamics

We first work out the case of two qubits explicitly and then present the result for an arbitrary number of qubits. The initial state is

$$|\Psi_0\rangle = \frac{|e,e\rangle + |g,g\rangle}{\sqrt{2}} \otimes |\alpha,\alpha\rangle, \tag{5.2.8}$$

and at a later time the state of the system will read.

$$|\Psi_t\rangle = \frac{1}{\sqrt{2}}\left(|e,\phi_0\rangle + |g,\phi_1\rangle\right) \otimes \left(|e,\phi_0\rangle + |g,\phi_1\rangle\right) + \frac{1}{\sqrt{2}}\left(|e,\phi_2\rangle + |g,\phi_3\rangle\right) \otimes \left(|e,\phi_2\rangle + |g,\phi_3\rangle\right)$$

To find the concurrence we need to find the following elements

$$
\begin{aligned}
2X_{ee,gg} =& \left[\langle\phi_1|\phi_0\rangle^2 + \langle\phi_1|\phi_2\rangle^2 + \langle\phi_3|\phi_0\rangle^2 + \langle\phi_3|\phi_2\rangle^2\right], \\
|X_{ee,gg}| =& \frac{1}{4}|I_1^2 + x^2 - y^2 - I_2^2|, \\
2X_{eg,eg} =& \langle\phi_0|\phi_0\rangle\langle\phi_1|\phi_1\rangle + \langle\phi_2|\phi_2\rangle\langle\phi_3|\phi_3\rangle + \langle\phi_0|\phi_2\rangle\langle\phi_1|\phi_3\rangle + \langle\phi_2|\phi_0\rangle\langle\phi_3|\phi_1\rangle, \\
|X_{eg,eg}| =& \frac{1}{4}(1 - x^2 + y^2).
\end{aligned}
$$

We note that $X_{eg,eg} = X_{ge,ge}$. Thus the concurrence is given by

$$C_2 = \max\{0, Q_2\} \tag{5.2.9}$$

$$Q_2 = \frac{1}{2}(I_1^2 + 2x^2 - 2y^2 - I_2^2 - 1). \tag{5.2.10}$$

Now we find the all-party concurrence for $N \geq 3$. The state of the system is given by

$$|\Psi\rangle_t = \frac{1}{\sqrt{2}}\big(\otimes^N|e,\alpha\rangle_t + \otimes^N|g,\alpha\rangle_t\big). \tag{5.2.11}$$

According to our approximation we only need to calculate one off-diagonal element:

$$2^{N+1}|X_{ee\cdots e,gg\cdots g}| = \left|(-i)^N((I_2 - y)^N + (I_2 + y)^N) + (I_1 - x)^N + (I_1 + x)^N\right|.$$

Next we calculate the diagonal elements:

$$
\begin{aligned}
2X_{e^{\otimes n}g^{\otimes m},e^{\otimes n}g^{\otimes m}} =& \frac{1}{2^{n+m}}[(iy)^{n+m}((-1)^n + (-1)^m)] \\
&+ \frac{1}{2^{n+m}}[(1+x)^n(1-x)^m + (1-x)^n(1+x)^m].
\end{aligned} \tag{5.2.12}
$$

This equation implies that $\langle e^{\otimes p}, g^{\otimes q}|\hat{X}|e^{\otimes p}, g^{\otimes q}\rangle = \langle g^{\otimes p}, e^{\otimes q}|\hat{X}|g^{\otimes p}, e^{\otimes q}\rangle$. Using the above equations and also the permutation symmetry of the problem we can find all the diagonal elements of the density matrix. This simplification confirms that the X-part of the state will always remain a GHZ-diagonal state. This has two consequences. First, the concurrence of a GHZ-diagonal state is directly proportional to the distance of that state to the set of biseparable states [75]. This enables us to draw a picture of the trajectory that the state traverses in the Hilbert space. Second, since these GHZ-diagonal states have only one non-zero anti-diagonal element, we can determine the full-separability of them [73]. We use this property to also comment about the

full-separability give an even more comprehensive picture about the movement of the quantum state in the Hilbert space.

Now we discuss the dynamics of the all-party entanglement. For $N = 3$, the all-party concurrence is given by

$$C_3 = \max\{0, Q_3\} \tag{5.2.13}$$

$$Q_3 = 2(|X_{eee,ggg}| - 3|X_{eeg,eeg}|) \tag{5.2.14}$$

$$|X_{eee,ggg}| = \frac{1}{8}\sqrt{(I_1^3 + 3I_1^2 x)^2 + (I_2^3 + 3I_2^2 y)^2} \tag{5.2.15}$$

$$|X_{eeg,eeg}| = \frac{1}{8}(1 - x^2). \tag{5.2.16}$$

We plot C_2 and C_3 as a function of time in Fig. 5.6. As expected the entanglement dies out rapidly with the initial collapse. At $gt = 2\pi\alpha$ entanglement revives to a small value. The maximum of this revival can be estimated from the above equations

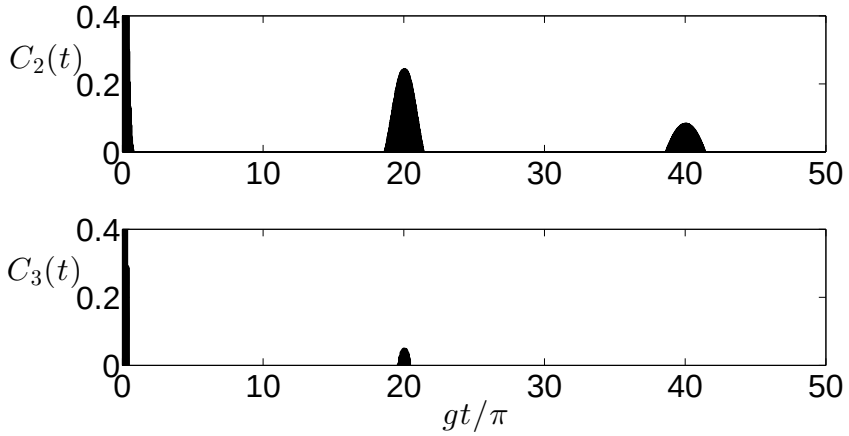

Figure 5.6: The revival of the entanglement for bipartite and genuinely tripartite entanglement for coherent states of $\alpha = 10$.

noting that the maximum value of x at first revival is $1/2$, and $I_1 \simeq -1$. At the revivals $I_2 \simeq 0$ and since x, y are completely out of phase with each other when x is at maximum revival, y vanishes. Feeding these quantities to the above equations leads to the maximum height of the bipartite and tripartite entanglement revivals to be $\frac{1}{4}$ and $\frac{1}{16}$ respectively. The second revival does not occur for tripartite entanglement. For $N > 3$ the sudden death of all-party entanglement is permanent. We emphasize that our two-qubit dynamics matches previous result derived in [90].

Dynamics of weak inseparability

Above we investigated the dynamics of the all-party entanglement. This is the kind of entanglement that implies inseparability of any part of the system from the rest. This is also the most fragile kind of inseparability. In the above case we saw that for $N > 3$ the all-party entanglement dies out permanently after the first collapse.

In the following we focus on another kind of inseparability; We study the inseparability in the sense that the state can not be written as a convex sum of fully separable states. All-party entanglement, which we studied so far, can be thought of as the most exclusive kind of entanglement whose presence implies that system is inseparable along any possible partitioning. Full separability is the other extreme of that line of thought whose presence implies that the system is separable along all possible partitioning. An N-party system is fully separable if it can be written as

$$\sum_i p_i \quad \rho_{1i} \otimes \rho_{2i} \otimes \cdots \otimes \rho_{Ni}. \tag{5.2.17}$$

So in a sense the onset of full separability is the true end of entanglement. In the following we follow the lack of full-separability that we refer to as weak inseparability. This will let us make a more complete picture of how the N-party system moves in the Hilbert space through out the dynamics.

To study the dynamics of inseparability we need to find a measure of weak inseparability. Here we use the distance of the state from the set of fully separable states as our measure of weak inseparability. In the previous chapter we showed that this distance is a proper measure of weak inseparability and we derived an algebraic formula for the weak inseparability of the GHZ-diagonal states that we are dealing with here. For the X-states for which all but one of anti-diagonal elements are zero and also $a_i = b_i$ we have shown that

$$S = 2\max\{0, |z_1| - c\} \tag{5.2.18}$$

where $c = \min\{b_i\}$. Below we plotted the value of this measure for $N = 3, 4, 5$. In all cases we see that inseparability revives back at around multiples of $gt = 2\pi\alpha$ until it decays away completely.

Finally we conclude with an attempt to capture the behavior of inseparability for large values of N. To this end we replace c in the inseparability formula with the

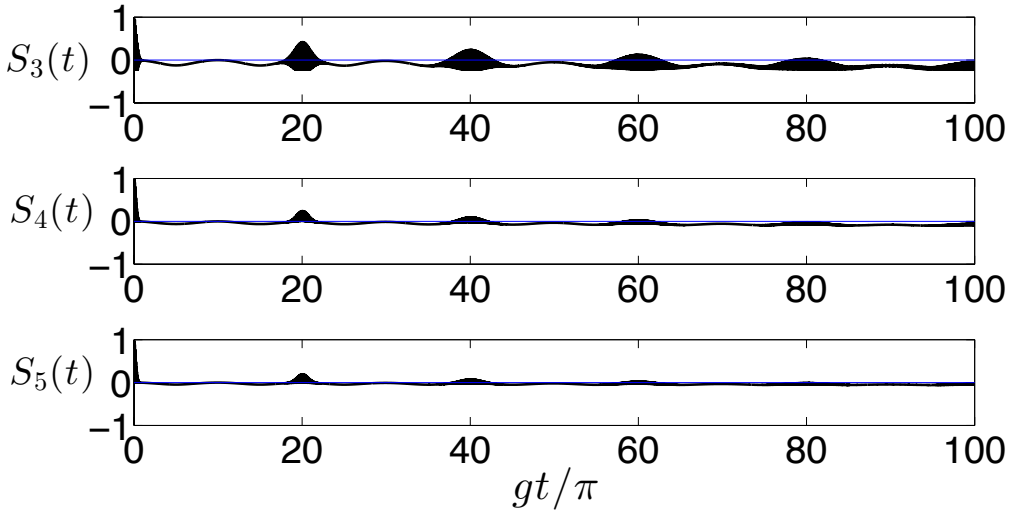

Figure 5.7: The revival of the inseparability for $N = 3, 4, 5$ for coherent states of $\alpha = 10$.

average values of all b_i's. we also assume that N is odd. Thus we can approximate

$$|z_1| = \frac{1}{2^{N+1}}[(|I_1| - x)^N + (|I_1| + x)^N] \tag{5.2.19}$$

$$2(n-1)b_i \simeq 1 - \frac{1}{2^N}[(1-x)^N + (1+x)^N] \tag{5.2.20}$$

For the first few revivals we can approximate $I_1 \simeq -1$ and thus derive

$$S_N \simeq \frac{1}{2^N}[(1-x)^N + (1+x)^N - 2] \tag{5.2.21}$$

This has a strong implication and that is at these revivals the inseparability revives back even for very large N. Yet its maximum distance from the boundary between fully separable and inseparable states decreases exponentially. For example at the first revival the maximum value of x is 0.5 and thus we can estimate $S_N \simeq (\frac{3}{4})^N$. Thus for large N the state follows a path to the boundary of inseparability and then stick below it crossing it momentarily only at revivals. The previous results and the fact that both of our measures have a geometrical interpretation suggest a picture for how the state moves in the Hilbert space [52]; In the Hilbert space there is a convex set that is the set of biseparable states, $\mathcal{BS}$. Inside this set there is another convex set which is the set of fully-separable states $\mathcal{FS}$. For $N = 2$ these two sets match. The

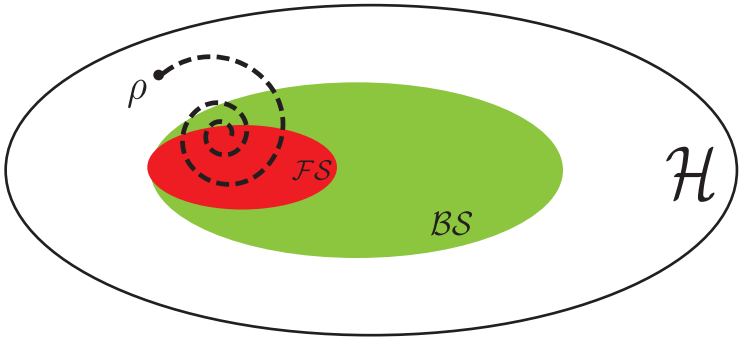

Figure 5.8: An schematic trajectory of the state in the Hilbert space for $N = 3$. $\mathcal{H}$, $\mathcal{BS}$, and $\mathcal{FS}$ stand for the Hilbert space, biseparable subspace and fully separable states respectively.

initial state start outside the $\mathcal{BS}$ and after five crossings it ends up inside $\mathcal{BS}$. For $N = 3$ the state starts outside $\mathcal{BS}$ and move inside $\mathcal{BS}$ and also $\mathcal{FS}$. At the first revival the state goes outside of both these sets and then comes back inside and gets trapped inside $\mathcal{BS}$ permanently. The state then moves inside $\mathcal{BS}$ crossing $\mathcal{FS}$ several times until it ends up somewhere in $\mathcal{FS}$. For $N \geq 4$, once inside the state never leaves $\mathcal{BS}$. It follows a trajectory that crosses $\mathcal{FS}$ several times and end up in $\mathcal{FS}$ finally. In Fig. 5.8 we have tried to capture these dynamics in the schematic plot.

Before closing this section let us summarize what is accomplished in this section. At the onset of this section we pointed out that current schemes of entanglement preservation do not simultaneously have many of the proper properties that one would desire. Here we have presented a concrete example of such an achievement. Our switching scheme enables us to turn the entanglement off and recover it partly at a controlled time. Our prescription includes simultaneously many of the desired aspects, namely mixed states, arbitrary number of qubits, quantitative measure, deterministic success, and external control.

5.3 Chapter summary

Quantifying the multipartite entanglement of a mixed states has remained an elusive challenge to tackle even now more than a century after its introduction in Schmidt's monumental achievement. The main theme of this chapter was to establish the utility of the all-party concurrence that we developed previously for X-states in deriving

analytical insights in a dynamical open systems, although it deals with the problem of entanglement in a restricted class of states.

In the first part of the chapter we used our formula to study the dynamics of all-party entanglement of N qubits interacting with their local amplitude damping channels. We diagnosed which GHZ states will experience the entanglement sudden death and which would only lose their entanglement asymptotically. Our calculations confirms that one should make distinction between the life-time when the state most the bulk of its entanglement versus the time when the state crosses the boundary of biseparability and becomes biseparable. The half-life of the all-party entanglement decreases as the number of qubits increases. Nevertheless, the time at which the state becomes biseparable does not necessarily decrease with N. We observe that In fact in the macroscopic limit $N \to \infty$, this time becomes independent of the initial state. We also presented a brief study on the robustness of all-party entanglement versus white noise. We observed that even for a very large number of qubits the all-party entanglement of a GHZ state is robust against white noise. Thus in an experimental settings one should care more about losing coherences to amplitude damping rather to mixedness with other states.

In the second part of the chapter we have used the machinery of quantifiable measures of entanglement that we have developed in the previous sections to present an example of taking advantage of phenomenon of coherent-state revivals to controllably suppress and recover the multipartite entanglement. We only studied two extreme kinds of entanglement, namely all-party entanglement and weak inseparability. All-party entanglement is so fragile that beyond three qubits it vanishes after its collapse it never recovers. On the other hand the, the weak inseparability always experiences a revival. Even for very large values of N, weak inseparability revives from zero before disappearing again. We comment that the strength of this revivals decrease as the number of qubits increases.

Finally, our results suggest a clear picture of how the state evolves and moves between different subset of the Hilbert space. If the system starts in a genuinely N-partite entangled state its evolution takes it back and forth over the boundary of biseparability and full-separability, ending up somewhere close to the boundary of full separability.

Appendix A

Multipartite entanglement in open systems

A.1 Detailed evaluations and approximations

In this section we calculate the inner products that we used previously to compute the elements of the density matrices.

$$\langle\phi_0|\phi_0\rangle = \sum_{n=0} A_n^2 |r_{n+1}|^2 \tag{A.1}$$

$$\langle\phi_1|\phi_1\rangle = \sum_{n=0} A_n^2 |t_{n+1}|^2 \tag{A.2}$$

$$\langle\phi_3|\phi_3\rangle = \sum_{n=0} A_n^2 |r_n|^2 \tag{A.3}$$

$$\langle\phi_2|\phi_2\rangle = \sum_{n=0} A_n^2 |t_n|^2 \tag{A.4}$$

The next two inner products are

$$\langle\phi_0|\phi_1\rangle = \sum_{n=0} A_{n+1} A_n r_{n+2}^* t_{n+1} \tag{A.5}$$

$$\langle\phi_2|\phi_3\rangle = \sum_{n=0} A_{n+1} A_n t_{n+1}^* r_n \tag{A.6}$$

and finally we have another four inner products

$$\langle\phi_0|\phi_2\rangle = \sum_{n=0} A_n A_{n+1} r^*_{n+1} t_{n+1} \tag{A.7}$$

$$\langle\phi_0|\phi_3\rangle = \sum_{n=0} A^2_n r^*_{n+1} r_n \tag{A.8}$$

$$\langle\phi_1|\phi_2\rangle = \sum_{n=0} A_n A_{n+2} t^*_{n+1} t_{n+2} \tag{A.9}$$

$$\langle\phi_1|\phi_3\rangle = \sum_{n=0} A_n A_{n+1} t^*_{n+1} r_{n+1} \tag{A.10}$$

We can compute the above inner products using appropriate approximations. The first term that we compute is $\langle\phi_2|\phi_2\rangle$.

$$\begin{aligned}\langle\phi_2|\phi_2\rangle =& \sum_{n=0} A^2_n |t_n|^2 = \sum_{n=0} A^2_n |\sin(gt\sqrt{n})|^2 \\ =& \frac{1}{2} - \frac{1}{2}\sum_{n=0} A^2_n \cos(2gt\sqrt{n})\end{aligned} \tag{A.11}$$

To evaluate the sum we use the approach developed in [97]. First we rewrite the sum using the Poisson sum formula.

$$\sum_{m=0}^{\infty} f_m = \sum_{\nu=-\infty}^{\infty} \int_0^{\infty} dm f(m) e^{2\pi i \nu m} + \frac{f_0}{2} \tag{A.12}$$

where $f(m)$ is a continuous version of f_m. First we follow the general formalism. In these integrals A^2_n is the Poisson distribution and it only contributes significantly when

$m \approx \alpha^2$ and it is the slowly varying factor. Thus we rewrite the sum in $\langle\phi_2|\phi_2\rangle$ as

$$
\begin{aligned}
&-\frac{1}{2}\sum_{m=0}^{\infty} A_m^2 \cos(2gt\sqrt{m}) \qquad (A.13)\\
&= -\frac{1}{2}\Re\left(\sum_{m=0}^{\infty} A_m^2 \exp(-2igt\sqrt{m})\right)\\
&= -\frac{1}{2}\Re\left(\sum_{\nu=-\infty}^{\infty}\int_0^{\infty} dmA(m)^2 e^{-2igt\sqrt{m}} e^{2\pi i\nu m} + \frac{A_0^2}{2}\right)\\
&= -\frac{1}{2}\Re\left(\sum_{\nu=-\infty}^{\infty}\int_0^{\infty} dmA(m)^2 e^{2iS_\nu(m)} + \frac{A_0^2}{2}\right)\\
&= \sum_{\nu=-\infty}^{\infty} w_\nu(t) + \frac{A_0^2}{2}
\end{aligned}
$$

where $S_\nu(m) = \pi\nu m - gt\sqrt{m}$. Now we can use the stationary phase approximation, a variation of saddle point approximation, to approximate these integrals. We approximate $S_\nu(m)$ around the point of stationary phase:

$$S_\nu(m) = S_\nu(m_\nu) + \frac{1}{2}\frac{\partial^2 S_\nu(m_\nu)}{\partial m^2}(m - m_\nu)^2. \qquad (A.14)$$

where $\frac{\partial S_\nu(m_\nu)}{\partial m} = 0$. Then we will have

$$w_\nu(t) = \frac{-A(m_\nu)^2}{2}\sqrt{\frac{\pi}{|\frac{\partial^2 S_\nu(m_\nu)}{\partial m^2}|}}\cos(2S_\nu(m_\nu) + \eta\frac{\pi}{4}) \qquad (A.15)$$

where $\eta = \mathrm{sgn}(\frac{\partial^2 S_\nu(m_\nu)}{\partial m^2})$. In the above case $m_\nu = \frac{g^2t^2}{4\pi^2\nu^2}$ and

$$S_\nu(m_\nu) = -\frac{g^2t^2}{4\pi\nu} \qquad (A.16)$$

$$\frac{\partial^2 S_\nu(m_\nu)}{\partial m^2} = \frac{2\pi^2\nu^3}{g^2t^2} > 0 \qquad (A.17)$$

$$w_\nu(t) = -\frac{1}{2}A(\frac{g^2t^2}{4\pi^2\nu^2})^2\left(\frac{gt}{\pi\sqrt{2\nu^3}}\right)\cos(\frac{g^2t^2}{2\pi\nu} - \frac{\pi}{4}) \qquad (A.18)$$

The photonic distribution in A_m^2 is translated to a series of distributions in time. Since we are interested in positive time, the $\nu = 0$ gives the collapse and $\nu > 0$ lead to different revivals. Note that for simplicity we can approximate A_m^2 with a Gaussian

distribution. This is an excellent approximation for moderately large values of $\alpha \geq 10$ that we are interested in here. If we use the above approximation we can conclude that

$$\begin{aligned} \langle \phi_3 | \phi_3 \rangle &= \sum_{n=0} A_n^2 |r_n|^2 = \frac{1+x}{2} \\ \langle \phi_2 | \phi_2 \rangle &= \sum_{n=0} A_n^2 |t_n|^2 = \frac{1-x}{2} \end{aligned} \tag{A.19}$$

where $x = \sum_{n=0} A_n^2 \cos(2gt\sqrt{n})$. We also approximate $A_n A_{n+1} = A_n^2$. With this approximation.

$$\begin{aligned} \langle \phi_3 | \phi_3 \rangle &= \langle \phi_0 | \phi_0 \rangle \\ \langle \phi_2 | \phi_2 \rangle &= \langle \phi_1 | \phi_1 \rangle \end{aligned} \tag{A.20}$$

If we define $y = \sum_{n=0} A_n^2 \sin(2gt\sqrt{n})$ we can estimate

$$\begin{aligned} \langle \phi_0 | \phi_2 \rangle =& \sum_{n=0} A_n A_{n+1} r_{n+1}^* t_{n+1} \qquad \text{(A.21)} \\ \simeq& -i \sum_{n=0} A_n^2 \cos(gt\sqrt{n}) \sin(gt\sqrt{n}) = \frac{-iy}{2} \\ \langle \phi_1 | \phi_3 \rangle \simeq \langle \phi_2 | \phi_0 \rangle =& \frac{iy}{2} \qquad \text{(A.22)} \end{aligned}$$

Now we have only four inner products to calculate and they are all related to each other. The simplest is

$$\begin{aligned} \langle \phi_0 | \phi_3 \rangle =& \sum_{n=0} A_n^2 r_{n+1}^* r_n \qquad \text{(A.23)} \\ =& e^{i\omega t} \sum_{n=0} A_n^2 \cos(gt\sqrt{n+1}) \cos(gt\sqrt{n}), \end{aligned}$$

and we can rewrite this quantity as

$$\begin{aligned}\langle\phi_0|\phi_3\rangle =&\frac{e^{i\omega t}}{2}\sum_{n=0}A_n^2\cos(gt\sqrt{n+1}+gt\sqrt{n})\\ &+\frac{e^{i\omega t}}{2}\sum_{n=0}A_n^2\cos(gt\sqrt{n+1}-gt\sqrt{n})\\ \simeq&\frac{e^{i\omega t}}{2}\sum_{n=0}A_n^2\cos(2gt\sqrt{n}+\frac{gt}{2\sqrt{n}})\\ &+\frac{e^{i\omega t}}{2}\sum_{n=0}A_n^2\cos(\frac{gt}{2\sqrt{n}}).\end{aligned}\tag{A.24}$$

Similarly we can get

$$\begin{aligned}\langle\phi_1|\phi_2\rangle =&\sum_{n=0}A_nA_{n+2}t_{n+1}^*t_{n+2}\\ \simeq&e^{-i\omega t}\sum_{n=0}A_n^2\sin(gt\sqrt{n+1})\sin(gt\sqrt{n})\\ \simeq&\frac{e^{-i\omega t}}{2}\sum_{n=0}A_n^2[\cos(\frac{gt}{2\sqrt{n}})-\cos(2gt\sqrt{n}+\frac{gt}{2\sqrt{n}})]\end{aligned}\tag{A.25}$$

and

$$\begin{aligned}\langle\phi_0|\phi_1\rangle =&\sum_{n=0}A_{n+1}A_nr_{n+2}^*t_{n+1}\\ \simeq&-ie^{i\omega t}\sum_{n=0}A_n^2\cos(gt\sqrt{n+1})\sin(gt\sqrt{n})\\ =&-i\frac{e^{i\omega t}}{2}\sum_{n=0}A_n^2[-\sin(\frac{gt}{2\sqrt{n}})+\sin(2gt\sqrt{n}+\frac{gt}{2\sqrt{n}})],\\ \langle\phi_2|\phi_3\rangle =&\sum_{n=0}A_{n+1}A_nt_{n+1}^*r_n\\ \simeq&ie^{i\omega t}\sum_{n=0}A_n^2\sin(gt\sqrt{n+1})\cos(gt\sqrt{n})\\ =&\frac{ie^{i\omega t}}{2}\sum_{n=0}A_n^2[\sin(\frac{gt}{2\sqrt{n}})+\sin(2gt\sqrt{n}+\frac{gt}{2\sqrt{n}})].\end{aligned}\tag{A.26}$$

Two of the above summations lead to evaluations of x, y that we already explained how to evaluate. The other two summations are evaluated in [90]. In the limit of

$\alpha^2 \gg 1$ we have

$$I = \sum_{n=0} A_n^2 \exp(\frac{igt}{2\sqrt{n}}) \simeq \exp(-\frac{g^2t^2}{32\alpha^4}) e^{\frac{igt}{2\alpha}} = I_1 + iI_2 \tag{A.27}$$

Bibliography

[1] E. Schrödinger, Proc. Cambridge Philos. Soc. **31**(04), 555 (1935).

[2] E. Schmidt, Math. Annalen **63**, 433 (1906).

[3] O. Gühne and G. Tóth, Phys. Rep. **474**(16), 1 (2009).

[4] R. Horodecki, P. l. Horodecki, M. l. Horodecki, and K. Horodecki, Rev. Mod. Phys. **81**(2), 865 (2009).

[5] M. A. Nielsen and I. L. Chuang, *Quantum Computation and Quanum Information* (Cambridge University Press, Cambridge, UK, 2000).

[6] V. Giovannetti, S. Lloyd, and L. Maccone, Science **306**(5700), 1330 (2004).

[7] J. T. Barreiro, P. Schindler, O. Gühne, T. Monz, M. Chwalla, C. F. Roos, M. Hennrich, and R. Blatt, Nature Physics **6**(12), 943 (2010).

[8] T. Monz, P. Schindler, J. T. Barreiro, M. Chwalla, D. Nigg, W. A. Coish, M. Harlander, W. H ansel, M. Hennrich, and R. Blatt, Phys. Rev. Lett. **106**, 130506 (2011).

[9] D. Bouwmeester, J.-W. Pan, M. Daniell, H. Weinfurter, and A. Zeilinger, Phys. Rev. Lett. **82**, 1345 (1999).

[10] C. A. Sackett, D. Kielpinski, B. E. King, C. Langer, V. Meyer, C. J. Myatt, M. Rowe, Q. A. Turchette, W. M. Itano, D. J. Wineland, *et al.*, Nature **404**(6775), 256 (2000).

[11] Z. Zhao, Y.-A. Chen, A.-N. Zhang, T. Yang, H. J. Briegel, and J.-W. Pan, Nature **430**(6995), 54 (2004).

[12] D. Leibfried, E. Knill, S. Seidelin, J. Britton, R. Blakestad, J. Chiaverini, D. Hume, W. Itano, J. Jost, C. Langer, *et al.*, Nature **438**(7068), 639 (2005).

[13] M. Rådmark, M. Żukowski, and M. Bourennane, Phys. Rev. Lett. **103**, 150501 (2009).

[14] W.-B. Gao, C.-Y. Lu, X.-C. Yao, P. Xu, O. Gühne, A. Goebel, Y.-A. Chen, C.-Z. Peng, Z.-B. Chen, and J.-W. Pan, Nature Physics **6**(5), 331 (2010).

[15] X.-C. Yao, T.-X. Wang, P. Xu, H. Lu, G.-S. Pan, X.-H. Bao, C.-Z. Peng, C.-Y. Lu, Y.-A. Chen, and J.-W. Pan, Nature Photonics **6**(4), 225 (2012).

[16] P. Hyllus, W. Laskowski, R. Krischek, C. Schwemmer, W. Wieczorek, H. Weinfurter, L. Pezzé, and A. Smerzi, Phys. Rev. A **85**, 022321 (2012).

[17] G. Tóth, Phys. Rev. A **85**, 022322 (Feb 2012).

[18] A. Peres, Phys. Rev. Lett. **77**, 1413 (Aug. 1996).

[19] M. Horodecki, P. Horodecki, and R. Horodecki, Phys. Lett. A **223**(1-2), 1 (1996).

[20] W. K. Wootters, Phys. Rev. Lett. **80**(10), 2245 (1998).

[21] B. M. Terhal and K. G. H. Vollbrecht, Phys. Rev. Lett. **85**, 2625 (Sep. 2000).

[22] P. Rungta and C. M. Caves, Phys. Rev. A **67**, 012307 (Jan. 2003).

[23] R. Lohmayer, A. Osterloh, J. Siewert, and A. Uhlmann, Phys. Rev. Lett. **97**, 260502 (2006).

[24] T.-C. Wei, Phys. Rev. A **78**, 012327 (Jul. 2008).

[25] O. Gühne and M. Seevinck, New Journal of Physics **12**(5), 053002 (2010).

[26] Z.-H. Ma, Z.-H. Chen, J.-L. Chen, C. Spengler, A. Gabriel, and M. Huber, Phys. Rev. A **83**, 062325 (Jun. 2011).

[27] S. a. Szalay, Phys. Rev. A **83**, 062337 (Jun. 2011).

[28] B. Jungnitsch, T. Moroder, and O. G uhne, Phys. Rev. Lett. **106**, 190502 (2011).

[29] L. Novo, T. Moroder, and O. Gühne, Phys. Rev. A **88**, 012305 (2013).

[30] C. Eltschka and J. Siewert, Phys. Rev. Lett. **108**, 020502 (2012).

[31] J. Siewert and C. Eltschka, Phys. Rev. Lett. **108**, 230502 (2012).

[32] S. M. Hashemi Rafsanjani, M. Huber, C. J. Broadbent, and J. H. Eberly, Phys. Rev. A **86**, 062303 (2012).

[33] J. B. Altepeter, D. F. V. James, and P. G. Kwiat, *Quantum State Estimation* (Springer, 2004), chap. 4. Qubit Quantum State Tomography, pp. 113–145.

[34] J. Eisert, F. Brandão, and K. Audenaert, New J. Phys. **9**(3), 46 (2007).

[35] O. Gühne, M. Reimpell, and R. F. Werner, Phys. Rev. Lett. **98**, 110502 (2007).

[36] A. Osterloh and P. Hyllus, Phys. Rev. A **81**, 022307 (2010).

[37] C. Eltschka and J. Siewert, Scientific Reports **2**, 942 (December 2012).

[38] G. Vidal, Journal of Modern Optics **47**, 355 (2000).

[39] C. H. Bennett, H. J. Bernstein, S. Popescu, and B. Schumacher, Phys. Rev. A **53**, 2046 (1996).

[40] S. Popescu and D. Rohrlich, Phys. Rev. A **56**, R3319 (1997).

[41] F. Mintert, *Measures and dynamics of entangled states*, Ph.D. thesis, Munich University (2004).

[42] L. P. Hughston, R. Jozsa, and W. K. Wootters, Physics Letters A **183**(1), 14 (1993).

[43] P. Rungta, V. Bužek, C. M. Caves, M. Hillery, and G. J. Milburn, Phys. Rev. A **64**, 042315 (Sep 2001).

[44] G. Vidal and R. F. Werner, Phys. Rev. A **65**, 032314 (2002).

[45] K. Modi, T. Paterek, W. Son, V. Vedral, and M. Williamson, Phys. Rev. Lett. **104**, 080501 (Feb. 2010).

[46] A. Gabriel, B. C. Hiesmayr, and M. Huber, Quantum Information & Computation **10**(9), 829 (2010).

[47] M. Huber, F. Mintert, A. Gabriel, and B. C. Hiesmayr, Phys. Rev. Lett. **104**, 210501 (May 2010).

[48] D. T. Pope and G. J. Milburn, Phys. Rev. A **67**, 052107 (May 2003).

[49] P. Love, A. van den Brink, A. Smirnov, M. Amin, M. Grajcar, E. Ilichev, A. Izmalkov, and A. Zagoskin, Quant. Inf. Proc. **6**, 187 (2007).

[50] J.-Y. Wu, H. Kampermann, D. Bru ss, C. Kl ockl, and M. Huber, Phys. Rev. A **86**, 022319 (2012).

[51] T. Yu and J. H. Eberly, Phys. Rev. Lett. **93**(14), 140404 (Sep. 2004).

[52] T. Yu and J. H. Eberly, Quantum Inf. Comput. **7**, 459 (2007).

[53] M. Yönaç, T. Yu, and J. H. Eberly, J. Phys. B: At. Mol. Opt. Phys. **39**(15), S621 (2006).

[54] M. Yönaç, T. Yu, and J. H. Eberly, J. Phys. B **40**(9), S45 (2007).

[55] H. T. Cui, K. Li, and X. X. Yi, Phys. Lett. A **365**(1-2), 44 (2007).

[56] G. Zhang and Z. Chen, Opt. Commun. **275**(1), 274 (2007).

[57] Z. Ficek and R. Tana ifmmode acute s else s fi, Phys. Rev. A **77**, 054301 (2008).

[58] A. Al-Qasimi and D. F. V. James, Phys. Rev. A **77**(1), 012117 (Jan. 2008).

[59] M. Ali, G. Alber, and A. R. P. Rau, Journal of Physics B: At. Mol. Opt. Phys. **42**(2), 025501 (2009).

[60] N. Quesada, A. Al-Qasimi, and D. F. V. James, Journal of Modern Optics **59**(15), 1322 (2012).

[61] A. Uhlmann, Phys. Rev. A **62**, 032307 (Aug. 2000).

[62] S. Albeverio and S. M. Fei, J. Opt. B: Quantum Semiclass. Opt. **3**, 223 (2001).

[63] S. Vinjanampathy and A. R. P. Rau, Phys. Rev. A **82**, 032336 (Sep. 2010).

[64] A. R. P. Rau, J. Phys. A **42**(41), 412002 (2009).

[65] O. Gühne, Phys. Lett. A **375**(3), 406 (2011).

[66] S. Ishizaka and T. Hiroshima, Phys. Rev. A **62**, 022310 (Jul. 2000).

[67] W. J. Munro, D. F. V. James, A. G. White, and P. G. Kwiat, Phys. Rev. A **64**, 030302 (Aug. 2001).

[68] F. Verstraete, K. Audenaert, and B. De Moor, Phys. Rev. A **64**, 012316 (Jun. 2001).

[69] S. R. Hedemann, arXiv preprint arXiv:1310.7038 (2013).

[70] P. E. Mendonça, M. A. Marchiolli, and D. Galetti, Annals of Physics **351**(0), 79 (2014).

[71] V. Vedral, M. B. Plenio, M. A. Rippin, and P. L. Knight, Phys. Rev. Lett. **78**, 2275 (Mar. 1997).

[72] S. Agarwal and S. M. Hashemi Rafsanjani, Int. J. Quant. Inf. **11**, 1350043 (2013).

[73] W. Dür and J. I. Cirac, Phys. Rev. A **61**, 042314 (2000).

[74] A. Kay, Phys. Rev. A **83**, 020303 (2011).

[75] S. M. Hashemi Rafsanjani, C. J. Broadbent, and J. H. Eberly, Phys. Rev. A **88**(6), 062331 (2013).

[76] S. M. Hashemi Rafsanjani, C. J. Broadbent, and J. H. Eberly, Phys. Rev. A **88**, 062331 (2013).

[77] R. F. Werner, Physical Review A **40**(8), 4277 (1989).

[78] L. Aolita, R. Chaves, D. Cavalcanti, A. Ac 'in, and L. Davidovich, Phys. Rev. Lett. **100**, 080501 (Feb. 2008).

[79] Z.-X. Man, Y.-J. Xia, and N. B. An, Journal of Physics B: At. Mol. Opt. Phys. **41**(15), 155501 (2008).

[80] Y. S. Weinstein, Phys. Rev. A **82**, 032326 (Sep. 2010).

[81] L. Aolita, D. Cavalcanti, A. Ac i n, A. Salles, M. Tiersch, A. Buchleitner, and F. de Melo, Phys. Rev. A **79**, 032322 (2009).

[82] Y. S. Weinstein, Phys. Rev. A **79**, 012318 (Jan. 2009).

[83] D. Gross, Y.-K. Liu, S. T. Flammia, S. Becker, and J. Eisert, Phys. Rev. Lett. **105**, 150401 (2010).

[84] M. Mirhosseini, O. S. Magaña Loaiza, S. M. Hashemi Rafsanjani, and R. W. Boyd, Phys. Rev. Lett. **113**, 090402 (2014).

[85] S. Maniscalco, F. Francica, R. L. Zaffino, N. Lo Gullo, and F. Plastina, Phys. Rev. Lett. **100**, 090503 (2008).

[86] P. G. Kwiat, S. Barraza-Lopez, A. Stefanov, and N. Gisin, Nature (2001).

[87] J.-W. Pan, S. Gasparoni, R. Ursin, G. Weihs, and A. Zeilinger, Nature (2003).

[88] R. Dong, M. Lassen, J. Heersink, C. Marquardt, R. Filip, G. Leuchs, and U. L. Andersen, Nat. Phys. (2008).

[89] Y.-S. Kim, J.-C. Lee, O. Kwon, and Y.-H. Kim, Nat. Phys. **8**, 117 (2012).

[90] M. Yönaç and J. H. Eberly, Phys. Rev. A **82**(2), 022321 (2010).

[91] J. Gea-Banacloche, Phys. Rev. Lett. **65**, 3385 (1990).

[92] S. J. D. Phoenix and P. L. Knight, Phys. Rev. A **44**, 6023 (1991).

[93] J. H. Eberly and J. J. Sanchez-Mondragon, Phys. Rev. Lett. **44**(20), 1323 (1980).

[94] E. T. Jaynes and F. W. Cummings, Proc. IEEE **51**(1), 89 (1963).

[95] B. Vlastakis, G. Kirchmair, Z. Leghtas, S. E. Nigg, L. Frunzio, S. M. Girvin, M. Mirrahimi, M. H. Devoret, and R. J. Schoelkopf, Science **342**(6158), 607 (2013).

[96] M. Yönaç and J. H. Eberly, Opt. Lett. **33**(3), 270 (Feb 2008).

[97] M. Fleischhauer and W. P. Schleich, Phys. Rev. A **47**, 4258 (1993).